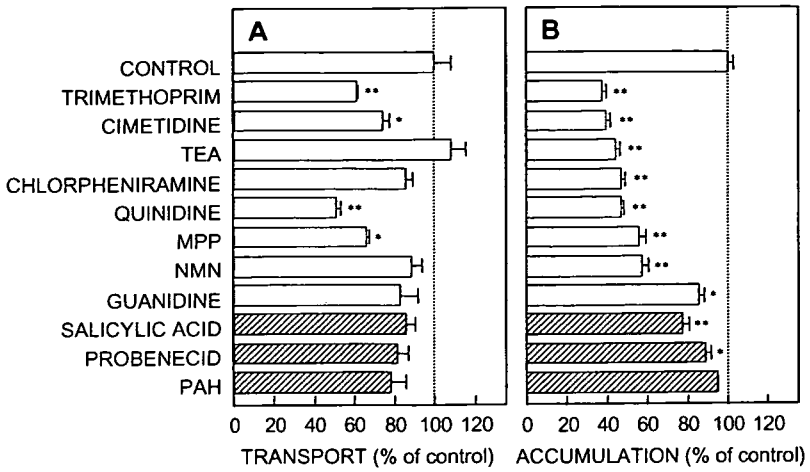

Fig. 4. Effect of organic cations and anions on the transcellular transport (A) and accumulation (B) of [^{14}C]creatinine in LLC-PK$_1$ cell monolayers. LLC-PK$_1$ cell monolayers were incubated at 37°C for 15 min with 5 μM [^{14}C]creatinine added to the basolateral side in the absence (control) or presence of cationic or anionic compounds (1 mM) on the basolateral side. The pHs of both basolateral and apical media were 7.4. MPP, 1-methyl-4-phenylpyridinium; NMN, N^1-methylnicotinamide; PAH, *p*-aminohippuric acid. Each column represents the mean ± S.E. for three monolayers from a typical experiment. *, $P<0.05$; **, $P<0.01$, significant difference from control using analysis of variance followed by Dunnett's test.

also inhibited significantly the accumulation of [^{14}C]creatinine from the basolateral side (**Fig. 4B**). Furthermore, guanidine, salicylic acid, and probenecid slightly inhibited the accumulation of [^{14}C]creatinine from the basolateral side (**Fig. 4B**). In contrast, *p*-aminohippuric acid had little inhibitory effect on both the transcellular transport (**Fig. 4A**) and accumulation (**Fig. 4B**).

Finally, we examined the effect of apical pH on the transcellular transport and accumulation of [^{14}C]creatinine. Both the transcellular transport (**Fig. 5A**) and accumulation (**Fig. 5B**) of [^{14}C]creatinine were mostly independent of the apical pH. In contrast, the transcellular transport of [^{14}C]TEA increased markedly with the acidification of the apical medium (**Fig. 5C**), as demonstrated by us.[11] Consistent with the increased extrusion of [^{14}C]TEA from the cells across apical membranes, the accumulation of [^{14}C]TEA decreased (**Fig. 5D**).

Discussion

Although organic ion transporters have been implicated in the tubular secretion of creatinine,[15,16] the characteristics of tubular secretion of creatinine have not been clarified. In the present study, we found that the transport of creatinine across LLC-PK$_1$ cell monolayers was directional from the basolateral to apical side (**Fig. 1**), and was markedly reduced in the presence of organic cations (**Fig. 4**), suggesting the involvement of organic cation transporters in the transcellular transport of creatinine. This is the first report to demonstrate the transcellular transport of creatinine *via* organic cation transport systems.

Several organic cation transporters (OCTs) have been identified.[5] hOCT2 is the dominant organic cation transporter in the human kidney,[17] and is driven by differences in membrane potential, mediating the basolateral uptake of organic cations into the renal epithelial cells. Recently, we demonstrated that creatinine was specifically transported by hOCT2, but not hOCT1 in the cDNA transfected HEK293 cells.[18] In the present study, the basolateral uptake of creatinine was dependent on the inside-negative membrane potential, being consistent with our previous findings. In addition, the apparent K_m value of the basolateral uptake of creatinine in LLC-PK$_1$ cells (13.2 ± 2.8 mM, **Fig. 2B**) was comparable to that in the hOCT2-expressing HEK293 cells (4.0 ± 0.3 mM).[18] Furthermore, the ability of various organic ions to inhibit the cellular accumulation of creatinine (**Fig. 4**) suggested that the creatinine uptake in LLC-PK$_1$ cells is mediated by an OCT-like transporter expressed at the basolateral membrane.

Acidification of the apical medium did not stimulate the elimination of creatinine from the cells, in contrast to the marked stimulation of apical excretion of TEA (**Fig. 5**). These results suggested that the contribution of the H^+/organic cation antiporter to the apical extrusion of creatinine is limited. Provided that the volume of LLC-PK$_1$ cells is 3.4 μL/mg protein,[19] the intracellular concentration of [^{14}C]creatinine after a 60-min incubation reached 7.4 μM (**Fig. 1B**), which was about 1.5-fold the extracellular concentration of [^{14}C]creatinine (5 μM). Taking into consideration that the accumulation of TEA was highly concentrative, i.e. 10-fold higher than that of extracellular [^{14}C]TEA (**Fig. 1D**), the transport of creatinine both at apical and basolateral

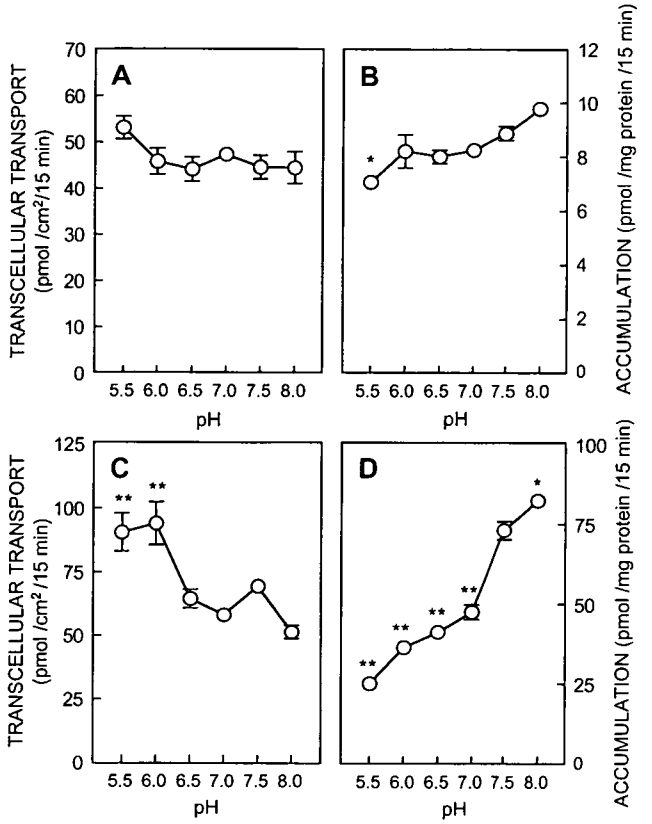

Fig. 5. Effect of apical pH on transcellular transport and accumulation of [^{14}C]creatinine (A and B) and [^{14}C]TEA (C and D) in LLC-PK$_1$ cell monolayers. LLC-PK$_1$ cell monolayers were incubated at 37°C for 15 min with 5 μM [^{14}C]creatinine or [^{14}C]TEA added to the basolateral side and apical media of various pH (5.5–8.0). The pH of the basolateral medium was 7.4. The radioactivity in the apical medium (A and C) and solubilized cells (B and D) was measured after incubation. Each point represents the mean ± S.E. for three monolayers from a typical experiment. *, $P<0.05$; **, $P<0.01$, significant difference from the value at pH 7.4 using analysis of variance followed by Dunnett's test. When error bars are not shown, they are included within the symbols.

membranes should be comparable with that of TEA.

In the present study, concomitant administration of cimetidine and trimethoprim significantly inhibited the creatinine transport across LLC-PK$_1$ cell monolayers (**Fig. 4**). It is reported that oral cimetidine administration improves the preciseness of GFR estimation due to the inhibition of tubular creatinine secretion in patients with renal diseases and renal transplant recipients.[16,20] In another study by Berglund *et al.*,[15] the serum creatinine level was elevated by a twice-daily administration of 160 mg of trimethoprim plus 800 mg of sulfamethoxazole through inhibition of the tubular secretion of creatinine. It is reported that a single oral dose of 200 mg of cimetidine to patients with normal renal function gave C_{max} values of between 2.3 μM and 6.8 μM,[21] which is lower than the IC_{50} value of cimetidine for the uptake of creatinine by hOCT2 (27 ± 6 μM).[18] On the other hand, the IC_{50} value of trimethoprim for the uptake of creatinine by hOCT2 (21 ± 2 μM) was marginal in view of the hOCT2-mediated transport of creatinine at therapeutic concentrations of trimethoprim.[18] Considering that a higher dose of cimetidine (800 mg daily) is used for the treatment of gastric and duodenal ulcers and reflux esophagitis and the systemic clearance of cimetidine and trimethoprim is delayed in patients with decreased renal functions. Concomitant administration of these drugs would interfere in part with the tubular secretion of creatinine via hOCT2 and increase the serum creatinine level.

In conclusion, we have demonstrated for the first time that transport of creatinine across renal epithelial cells was directional from the basolateral to apical side. These observations are relevant for understanding the molecular mechanisms underlying the tubular secretion of creatinine.

Acknowledgements: This work was supported in part by a grant-in-aid for Comprehensive Research on Aging and Health from the Ministry of Health, Labor and Welfare of Japan, a grant-in-aid for Scientific Research from the Ministry of Education, Science, Culture and Sports of Japan, and by the 21st Century COE program "Knowledge Information Infrastructure for Genome Science".

References

1) Kasiske, B. L. and Keane, W. F.: Laboratory assessment of renal disease: clearance, urinalysis, and renal biopsy. in Brenner, B. M. (ed): *The kidney*. W. B. Saunders, Philadelphia, PA, USA, 2000, pp. 1129–1170.
2) Sjostrom, P. A., Odlind, B. G. and Wolgast, M.: Extensive tubular secretion and reabsorption of creatinine in humans. *Scand. J. Urol. Nephrol.*, **22**: 129–131 (1988).
3) Shemesh, O., Golbetz, H., Kriss, J. P. and Myers, B. D.: Limitations of creatinine as a filtration marker in glomerulopathic patients. *Kidney Int.*, **28**: 830–838 (1985).
4) Inui, K. and Okuda, M.: Cellular and molecular mechanisms of renal tubular secretion of organic anions and cations. *Clin. Exper. Nephrol.*, **2**: 100–108 (1998).
5) Inui, K., Masuda, S. and Saito, H.: Cellular and molecular aspects of drug transport in the kidney. *Kidney Int.*, **58**: 944–958 (2000).
6) Koepsell, H.: Organic cation transporters in intestine, kidney, liver, and brain. *Annu. Rev. Physiol.*, **60**: 243–266 (1998).
7) Pritchard, J. B. and Miller, D. S.: Mechanisms mediating renal secretion of organic anions and cations. *Physiol. Rev.*, **73**: 765–796 (1993).
8) Takano, M., Inui, K., Okano, T., Saito, H. and Hori, R.: Carrier-mediated transport systems of tetraethylammonium in rat renal brush-border and basolateral membrane vesicles. *Biochim. Biophys. Acta.*, **773**: 113–124 (1984).

9) Wright, S. H.: Transport of N^1-methylnicotinamide across brush border membrane vesicles from rabbit kidney. *Am. J. Physiol.*, **249**: F903-F911 (1985).
10) Inui, K., Saito, H. and Hori, R.: H^+-gradient-dependent active transport of tetraethylammonium cation in apical-membrane vesicles isolated from kidney epithelial cell line LLC-PK_1. *Biochem. J.*, **227**: 199-203 (1985).
11) Saito, H., Yamamoto, M., Inui, K. and Hori, R.: Transcellular transport of organic cation across monolayers of kidney epithelial cell line LLC-PK_1. *Am. J. Physiol.*, **262**: C59-C66 (1992).
12) Ohtomo, T., Saito, H., Inotsume, N., Yasuhara, M. and Inui, K.: Transport of levofloxacin in a kidney epithelial cell line, LLC-PK_1: interaction with organic cation transporters in apical and basolateral membranes. *J. Pharmacol. Exp. Ther.*, **276**: 1143-1148 (1996).
13) Takami, K., Saito, H., Okuda, M., Takano, M. and Inui, K.: Distinct characteristics of transcellular transport between nicotine and tetraethylammonium in LLC-PK_1 cells. *J. Pharmacol. Exp. Ther.*, **286**: 676-680 (1998).
14) Bradford, M. M.: A rapid and sensitive method for the quantitation of microgram quantities of protein utilizing the principle of protein-dye binding. *Anal. Biochem.*, **72**: 248-254 (1976).
15) Berglund, F., Killander, J. and Pompeius, R.: Effect of trimethoprim-sulfamethoxazole on the renal excretion of creatinine in man. *J. Urol.*, **114**: 802-808 (1975).
16) van Acker, B. A. C., Koomen, G. C. M., Koopman, M. G., de Waart, D. R. and Arisz, L.: Creatinine clearance during cimetidine administration for measurement of glomerular filtration rate. *Lancet*, **340**: 1326-1329 (1992).
17) Motohashi, H., Sakurai, Y., Saito, H., Masuda, S., Urakami, Y., Goto, M., Fukatsu, A., Ogawa, O. and Inui, K.: Gene expression levels and immunolocalization of organic ion transporters in the human kidney. *J. Am. Soc. Nephrol.*, **13**: 866-874 (2002).
18) Urakami, Y., Kimura, N., Okuda, M. and Inui, K.: Creatinine transport by basolateral organic cation transporter hOCT2 in the human kidney. *Pharm. Res.*, **21**: 976-981 (2004).
19) Tomita, Y., Otsuki, Y., Hashimoto, Y. and Inui, K.: Kinetic analysis of tetraethylammonium transport in the kidney epithelial cell line, LLC-PK_1. *Pharm. Res.*, **14**: 1236-1240 (1997).
20) Kemperman, F. A., Surachno, J., Krediet, R. T. and Arisz, L.: Cimetidine improves prediction of the glomerular filtration rate by the Cockcroft-Gault formula in renal transplant recipients. *Transplantation*, **73**: 770-774 (2002).
21) Larsson, R., Bodemar, G. and Norlander, B.: Oral absorption of cimetidine and its clearance in patients with renal failure. *Eur. J. Clin. Pharmacol.*, **15**: 153-157 (1979).

Am J Physiol Gastrointest Liver Physiol 289: G471–G477, 2005.
First published May 19, 2005; doi:10.1152/ajpgi.00025.2005.

Characterization of the human peptide transporter PEPT1 promoter: Sp1 functions as a basal transcriptional regulator of human PEPT1

Jin Shimakura, Tomohiro Terada, Toshiya Katsura, and Ken-Ichi Inui

Department of Pharmacy, Kyoto University Hospital, Faculty of Medicine, Kyoto University, Sakyo-ku, Japan

Submitted 24 January 2005; accepted in final form 12 May 2005

Shimakura, Jin, Tomohiro Terada, Toshiya Katsura, and Ken-Ichi Inui. Characterization of the human peptide transporter PEPT1 promoter: Sp1 functions as a basal transcriptional regulator of human PEPT1. *Am J Physiol Gastrointest Liver Physiol* 289: G471–G477, 2005. First published May 19, 2005; doi:10.1152/ajpgi.00025.2005.— H^+-coupled peptide transporter 1 (PEPT1, SLC15A1) localized at the brush-border membranes of intestinal epithelial cells plays an important role in the intestinal absorption of small peptides and a variety of peptidemimetic drugs. PEPT1 is regulated by various factors, including hormones, dietary conditions, some pharmaceutics, and diurnal rhythm. But there is little information about the transcriptional regulation of PEPT1. In the present study, therefore, we cloned the human (h)PEPT1 promoter region and examined its promoter activity using a human intestinal cell line, Caco-2. Deletion analysis of the hPEPT1 promoter suggested that the region spanning −172 to −35 bp was essential for basal transcriptional activity. This region lacked a TATA-box but contained some GC-rich sites that supposedly bind with the transcription factor Sp1. Mutational analysis revealed that three of these putative Sp1 sites contributed to the transcriptional activity. EMSA showed that Sp1 bound to two GC-rich sites. Furthermore, inhibition of Sp1 binding by mithramycin A treatment significantly reduced the transcriptional activity. Finally, overexpression of Sp1 increased the transcriptional activity in a dose-dependent manner. This study reports the first characterization of the hPEPT1 promoter and shows the significant role of Sp1 in the basal transcriptional regulation of hPEPT1.

Caco-2; SLC15A1; small intestine

DIETARY PROTEINS ARE DEGRADATED into a mixture of free amino acids and small peptides. Cellular uptake of di- and tripeptides is mediated by H^+-coupled peptide transporter 1 (PEPT1, SLC15A1) located at the brush-border membranes of intestinal epithelial cells (8). Because of its broad substrate specificity, PEPT1 can accept several peptidelike drugs such as oral β-lactam antibiotics, the anticancer agent bestatin, and angiotensin-converting enzyme inhibitors (28). Thus PEPT1 plays important roles not only as a nutrient transporter but also as a drug transporter. It has been reported that intestinal PEPT1 is regulated by various factors (1), including hormones [insulin (11), thyroid hormone (2)], epidermal growth factor (18), cytokine (interferon-γ) (7), dietary conditions (17, 24), some pharmacological agents (3, 10), and diurnal rhythm (19). Although the elucidation of these regulatory mechanisms is quite important for nutritional therapy for absorptive disorders and for the efficient oral delivery of peptidelike drugs in a clinical situation, studies that address this point are limited. Shiraga et al. (24) has cloned the 5′-flanking region of rat PEPT1 and revealed that the rat PEPT1 promoter was transcriptionally regulated by some amino acids via the amino acid responsible element. In the mouse PEPT1 promoter, a functional promoter analysis demonstrated that essential promoter/enhancer sites were present within 1140 bp upstream of the transcription start site (9). Nevertheless, *cis* elements and/or *trans* factors, which are critical for basal transcriptional regulation, have not been identified in these studies. As for human (h)PEPT1, a computational sequence analysis but not a functional analysis has been conducted (29).

In the present study, to fully understand the transcriptional regulation of PEPT1, we cloned the 5′-flanking region of the hPEPT1 gene and identified the minimal region and *cis*-regulatory elements required for the basal hPEPT1 promoter activity. In addition, the results provide evidence for the involvement of Sp1 in the regulation of basal promoter activity.

MATERIALS AND METHODS

Materials. γ-[^{32}P]ATP was obtained from Amersham Biosciences (Buckinghamshire, UK). Anti-human Sp1 was purchased from Upstate (Charlottesville, VA). Restriction enzymes were from New England BioLabs (Beverly, MA). Mithramycin A was purchased from Sigma-Aldrich (St. Louis, MO). CMV-Sp1 plasmid was kindly provided by Dr. Robert Tjian (University of California, Berkeley, CA). All other chemicals used were of the highest purity available.

Cloning of the 5′-regulatory region of hPEPT1 gene. The 2940-bp flanking region upstream of the transcription start site, which was indicated in the literature (29), was cloned using primers (hPT1proSacI-F, hPT1proXhoI-R) shown in Table 1 and human genomic DNA (Promega, Madison, WI). The primers were designed based on the genomic sequence deposited in the literature (29). The PCR conditions were denaturing at 95°C for 5 min, followed by 30 cycles of denaturing at 95°C for 1 min, annealing at 60°C for 1 min, and extension at 72°C for 4 min, before a final extension at 72°C for 10 min. The PCR product was isolated by electrophoresis and subcloned into the firefly luciferase reporter vector, pGL3-Basic (Promega), at *Sac*I and *Xho*I sites. This full-length reporter plasmid is hereafter referred to as −2940/+60.

Preparation of deletion reporter constructs. The 5′-deleted constructs (−1111/+60, −960/+60, −401/+60, −247/+60, −172/+60, −89/+60, −21/+60 constructs) were generated by digestion of the −2940/+60 construct with *Hin*dIII and each of the following enzymes: *Nhe*I, *Kpn*I, *Psh*AI, *Pvu*II, *Apa*I, *Xma*I, and *Aat*II, respectively. The ends were blunted with T4 DNA polymerase and then self-ligated. The −35/+60 construct was generated by PCR with primers containing a *Sac*I site and *Xho*I site (Table 1). The site-directed mutations in putative Sp1-binding sites were introduced into the −172/+60 construct with a Quik Change XL site-directed mutagenesis kit (Stratagene, La Jolla, CA) with the primers listed in Table 1. The nucleotide sequences of these deleted or mutated constructs were

Address for reprint requests and other correspondence: Ken-ichi Inui, Dept. of Pharmacy, Kyoto Univ. Hospital, Sakyo-ku, Kyoto 606-8507, Japan (e-mail: inui@kuhp.kyoto-u.ac.jp).

The costs of publication of this article were defrayed in part by the payment of page charges. The article must therefore be hereby marked "*advertisement*" in accordance with 18 U.S.C. Section 1734 solely to indicate this fact.

0193-1857/05 $8.00 Copyright © 2005 the American Physiological Society

Table 1. *Oligonucleotide sequences of primers*

Name	Sequence (5′-3′)	Position
Primers for cloning of the hPEPT1 promoter		
hPEPT1proSacI-F	AGGAGCTCTTTCTCCCTAGGCACCACAGT	−2940 to −2920
hPEPT1proXhoI-R	AGCTCGAGCCATGGCGGCGGCTCCCAGGG	+60 to +40
Primers for the −35/+60 deletion construct		
hPEPT1pro-35SacI-F	AGGAGCTCCGGGGCCGGGCCTGGA	−35 to −20
hPEPT1proXhoI-R	AGCTCGAGCCATGGCGGCGGCTCCCAGGG	+60 to +40
Primers for the site-directed mutagenesis		
Mut A-F	GGTGGAGCCGGCGAACCCAACTCGCAGAGCTGGG	−85 to −52
Mut A-R	CCCAGCTCTGCGAGTTGGGTTCGCCGGCTCCACC	−85 to −52
Mut B-F	CACCGCCCCCCGAATGGATCCGGCGGCCCCG	−97 to −67
Mut B-R	CGGGGCCGCCGGATCCATTCGGGGGCGGTG	−97 to −67
Mut C-F	CTCCCCGCAGCACCGAACTCCGGGTGGAG	−107 to −79
Mut C-R	CTCCACCCGGAGTTCGGTGCTGCGGGGAG	−107 to −79
Mut D-F	CACCCGCACCTGAACCAAGGCTGGTGTCCACGCGC	−167 to −133
Mut D-R	GCGCGTGGACACCAGCCTTGGTTCAGGTGCGGGTG	−167 to −133
Oligonucleotide for EMSA		
Probe(−77/−54)-F1	CGGCGGCCCCGCCTCGCAGAGCTG	−77 to −54
Probe(−77/−54)-R1	CAGCTCTGCGAGGCGGGGCCGCCG	−77 to −54
Mut A-F1	CGGCGAACCCAACTCGCAGAGCTG	−77 to −54
Mut A-R1	CAGCTCTGCGAGTTGGGTTCGCCG	−77 to −54
Probe(−102/−75)-F1	CGCAGCACCGCCCCCCGGGTGGAGCCGG	−102 to −75
Probe(−102/−75)-R1	CCGGCTCCACCCGGGGGGCGGTGCTGCG	−102 to −75
Mut B-F1	CGCAGCACCGCCCCCCGAATGGATCCGG	−102 to −75
Mut B-R1	CCGGATCCATTCGGGGGGCGGTGCTGCG	−102 to −75
Mut C-F1	CGCAGCACCGAACTCCGGGTGGAGCCGG	−102 to −75
Mut C-R1	CCGGCTCCACCCGGAGTTCGGTGCTGCG	−102 to −75
Sp1-consensus-F1	ATTCGATCGGGGCGGGGCGAGC	
Sp1-consensus-R1	GCTCGCCCCGCCCCGATCGAAT	

*Sac*I and *Xho*I sites are underlined. Mutations introduced into the oligonucleotides are shown in bold. hPEPT1, human peptide transporter; Mut, mutation.

confirmed using a multicapillary DNA sequencer RISA384 system (Shimadzu, Kyoto, Japan).

Cell culture, transfection, and reporter gene assay. Caco-2 cells were obtained from the American Type Culture Collection (ATCC CRL-1392) and maintained in Dulbecco's modified Eagle's medium supplemented with 10% fetal bovine serum and 1% nonessential amino acids. Caco-2 cells were plated into 24-well plates (3×10^5 cells/well) and transfected the following day with the reporter constructs and 2.5 ng of the *Renilla reniformis* vector pRL-TK (Promega) using Lipofectamine 2000 (Invitrogen Japan KK, Tokyo, Japan) according to the manufacturer's recommendation. The medium was changed after 24 h. The firefly and *Renilla* activities were determined 48 h after the transfection using a dual luciferase assay kit (Promega) and a LB940 luminometer (Berthold, Bad Wildbad, Germany). The firefly activity was normalized to *Renilla* activity except for the CMV-Sp1 overexpression, which significantly stimulated the *Renilla* activity. For the inhibition experiment with mithramycin A, Caco-2 cells were treated with 50, 100, and 250 nM of mithramycin A at the time of transfection of the reporter constructs.

EMSA. Nuclear extract (NE) was prepared from Caco-2 cells grown in 60-mm culture dishes for 16 days. Cells were scraped off, suspended in 0.5 ml PBS, and centrifuged at 4°C and 1,500 *g* for 5 min. The cells were resuspended in 0.4 ml of a low-salt buffer [in mM: 10 HEPES (pH 7.9), 10 KCl, 0.1 EDTA, 0.1 EGTA, 1 DTT, and 0.5 PMSF, with 1% protease inhibitor cocktail (Nacalai tesque, Kyoto, Japan)] and incubated on ice for 15 min. After 50 μl of Nonidet P-40 were added, the tube was vigorously vortexed for 10 s and centrifuged at 4°C and 20,000 *g* for 5 min. The supernatant was removed and the nuclear pellet was resuspended in 50 μl of a high-salt buffer [in mM: 20 HEPES (pH 7.9), 400 NaCl, 1 EDTA, 1 EGTA, 1 DTT, and 1 PMSF, with 1% protease inhibitor cocktail], and the tube was vigorously shaken (250 rpm) at 4°C for 30 min. The tube was centrifuged at 4°C and 20,000 *g* for 5 min, and the supernatant was recovered.

The probes shown in Table 1 were prepared by annealing complementary sense and antisense oligonucleotides, followed by end-labeling with γ-[^{32}P]ATP using T4 polynucleotide kinase (Takara Bio, Otsu, Japan) and purification through a Sephadex G-25 column (Amersham Biosciences). EMSAs were performed according to the instructions for the Gel shift assay system (Promega). The binding mixture consisted of 1 μg Caco-2 nuclear extract, 0.5 μg poly(dI-dC), and unlabeled competitor probes in buffer solution containing (in mM) 10 Tris·HCl (pH 7.5), 50 NaCl, 1 $MgCl_2$, 0.5 EDTA, and 0.5 DTT, with 4% glycerol. After preincubation at room temperature for 10 min, labeled probes (~0.4 ng) were added and the binding mixture was incubated for a further 20 min. For supershift assays, 1 μg Sp1 antibody was added 10 min before the addition of the labeled probes. The volume of the binding mixture was 10 μl throughout the experiment. The DNA-protein complex was then separated on a 4% polyacrylamide gel at room temperature in 0.5 × Tris-borate-EDTA buffer. The gels were dried and exposed to X-ray film for autoradiography.

Data analysis. The results were expressed relative to the pGL3-Basic vector set at 1 except for the Sp1 overexpression experiment and represent the means ± SE of three replicates. Two or three experiments were conducted, and representative results were shown. In the mutational, Sp1 overexpression and inhibition experiments, statistical analysis was performed with the one-way ANOVA followed by Scheffé's *F*-post hoc testing.

RESULTS

Determination of minimal hPEPT1 promoter. To determine the minimal region required for basal activity of the promoter, a series of deletion constructs was transfected into Caco-2 cells and luciferase activity was measured (Fig. 1). The transfection with the longest reporter constructs (−2940/+60) resulted in a three- to fourfold-increase in luciferase activity compared with

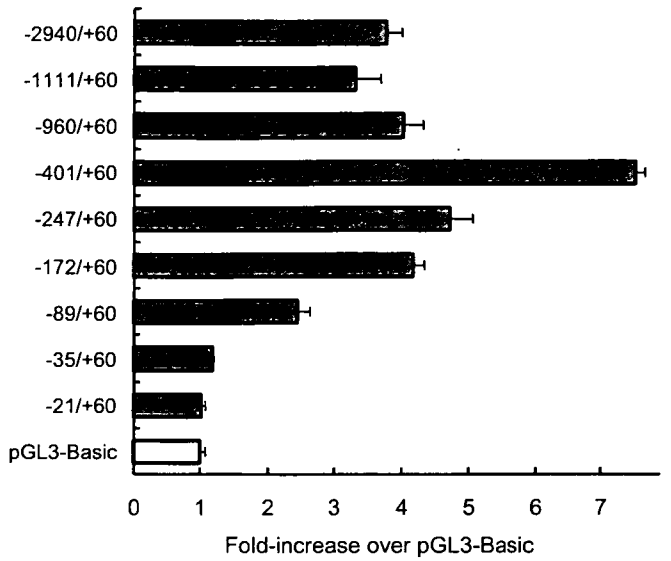

Fig. 1. Identification of transcriptional activity and deletion analysis of the human peptide transporter (hPEPT1) promoter in Caco-2 cells. A series of deleted promoter constructs [equimolar amounts of the −2940/+60 construct (500 ng)] were transfected into Caco-2 cells for luciferase assays. Firefly luciferase activity was normalized to *Renilla* luciferase activity. Data are reported as the relative fold increase compared with pGL3-Basic vector and represent the means ± SE of 3 replicates.

pGL3-Basic. The −1111/+60 construct reduced luciferase activity, suggesting the existence of some positive regulatory sites between −2940 and −1111. Deletion of the sequence from nucleotides −1111 to −960 and further deletion from −960 to −401 resulted in an increase in promoter activity, suggesting the presence of repressive elements in these regions. The −401/+60 construct had the strongest promoter activity, i.e., a sixfold increase in luciferase activity compared with pGL3-Basic. Serial 5′-deletions of the construct from −401 to −247, −172, −89, and −35 gradually reduced the activity, which was completely abolished with the −35/+60 construct. Thus the elements important for the basal promoter activity were shown to be located between −401 and −35. We considered the region between −172 and −35 to be the minimal promoter, because the −172/+60 construct retained fourfold greater activity than pGL3-Basic, which is almost the same level of activity as the longest construct, −2940/+60.

We performed a computational sequence analysis on the −401/−1 region of the hPEPT1 promoter, which had the strongest activity, using TFSEARCH at www.cbrc.jp/research/db/TFSEARCH.html (Fig. 2). This analysis revealed that the region proximal to the transcription start site lacks canonical TATA or CAAT boxes. Instead, several GC-rich sites were observed, suggesting a possible contribution of Sp1 to the transcriptional regulation of hPEPT1. This promoter region also had putative binding sites for AP-1, CREB, myeloid zinc finger 1, and caudal-related homeobox transcription factor Cdx A. Considering that the minimal regulatory elements are located downstream of −172, we subsequently focused on these putative Sp1-binding sites between −172 and −35.

Mutagenesis of the Sp1 sites. The putative Sp1-binding sites located between −172 and −35 were designated Sp-A, Sp-B, Sp-C, and Sp-D, as shown in Fig. 3*A*. To determine whether these sites were important for hPEPT1 promoter activity, mutations in these sites (*mut A*, *mut B*, *mut C*, and *mut D*, respectively) were introduced in the −172/+60 construct (Fig. 3*A*) and transfected into Caco-2 cells. As shown in Fig. 3*B*, *mut A* reduced the luciferase activity to one-third of the wild-type (WT) level. The luciferase activity was also markedly reduced by introducing *mut B* or *C*, whereas little effect was observed with *mut D*. These results suggest that the Sp-A, -B, and -C sites play an important role in regulating the hPEPT1 promoter activity.

EMSA. Next, we performed an EMSA using two oligonucleotide probes, *probe −77/−54* and *probe −102/−75*, and nuclear extract from Caco-2 cells to determine directly whether Sp1 binds to the promoter. *Probe −77/−54* formed three DNA-protein complexes, that is, complex I, II, and III, with the

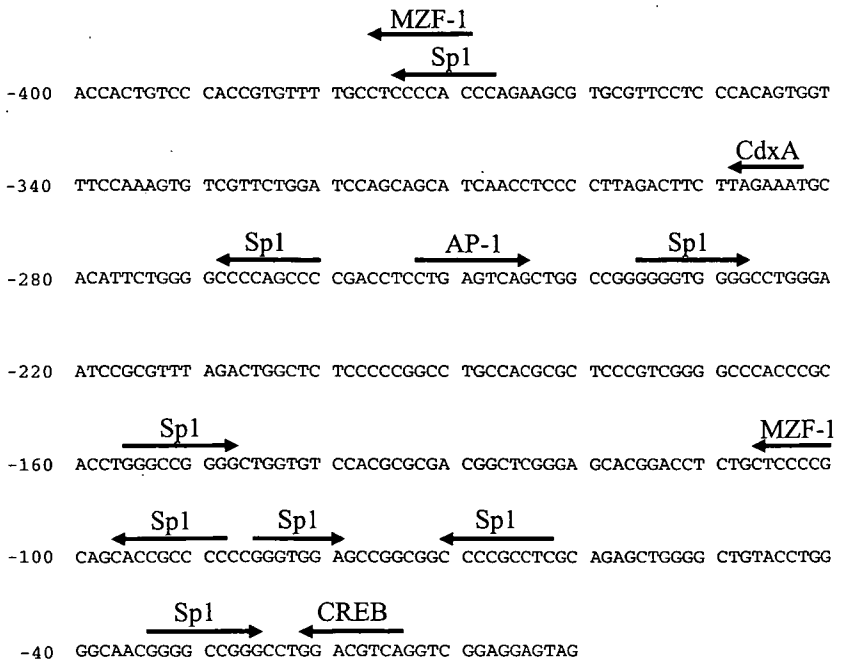

Fig. 2. Nucleotides sequence of the promoter region (−401 to −1) that had the highest basal activity. Numbering is relative to the transcription start site. The putative binding sites for the transcription factors are indicated on the sequence (the arrows indicate the direction). MZF-1, myeloid zinc finger 1.

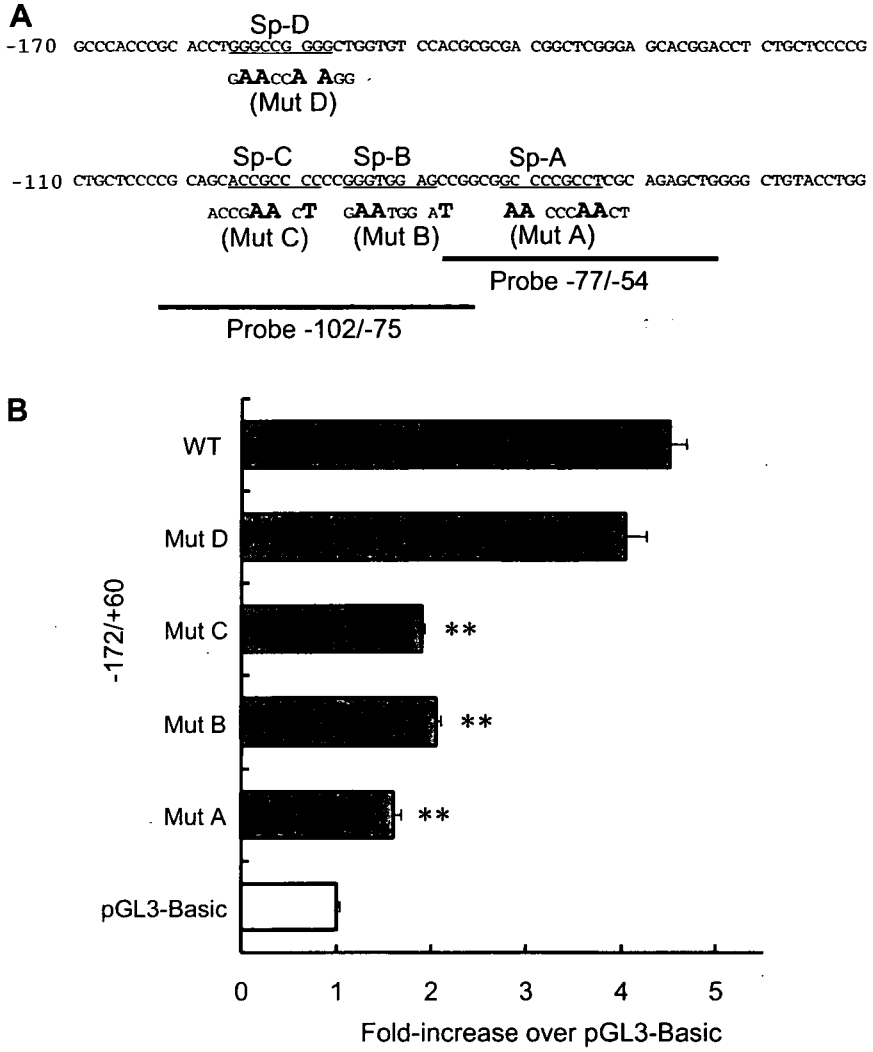

Fig. 3. Mutational analysis of the putative Sp1-binding elements of the hPEPT1 promoter. *A*: the nucleotide sequence of the promoter region of −170 to −41 is shown with the putative Sp1-binding elements (Sp-A, Sp-B, Sp-C, and Sp-D, underlined). Site-directed mutations that destroy Sp1-binding elements were introduced individually and designated *mut A*, *mut B*, *mut C*, and *mut D*. The nucleotides altered for mutational analysis are shown in bold under the wild-type (WT) sequence. The regions used for oligonucleotide probes for EMSA are also indicated. *B*: the mutated −172/+60 constructs (500 ng) were transiently expressed in Caco-2 cells for luciferase assays. Firefly luciferase activity was normalized to *Renilla* luciferase activity. Data are reported as the relative fold increase compared with pGL3-Basic vector and represent the means ± SE of 3 replicates. **Significantly different from WT ($P < 0.01$).

nuclear extract, whereas no complex was formed in the absence of nuclear extract (Fig. 4, *lanes 1* and *2*). The formation of all three complexes was completely competed away by the addition of an excess amount of unlabeled WT oligonucleotide but not by the *mut A* oligonucleotide (Fig. 4, *lanes 3* and *4*), suggesting that all these complexes bind to the Sp-A site. Moreover, Sp1 oligonucleotide competed the formation of complex I and II (Fig. 4, *lane 5*), further suggesting the identity of these factors as Sp1-like proteins. Sp1 appeared to exist in complex I because of the reduction of corresponding band and formation of supershifted band on incubation with anti-Sp1 antibody (Fig. 4, *lane 6*).

Probe −102/−75 formed three DNA-protein complexes (complexes IV, V, and VI) with the nuclear extract, whereas no complex was formed in the absence of nuclear extract (Fig. 4, *lanes 7* and *8*). The formation of the complex IV was completely diminished by the addition of an excess amount of unlabeled WT or *mut B* oligonucleotide but not by *mut C* oligonucleotide (Fig. 4, *lanes 9–11*). These results suggest that Sp-C is a more important region because the *mut B* oligonucleotide retains an intact Sp-C site, whereas the *mut C* oligonucleotide retains an intact Sp-B site. Complex IV was also competed by the addition of Sp1 consensus oligonucleotide and, most importantly, formed a supershifted band on incubation with anti-Sp1 antibody (Fig. 4, *lanes 12* and *13*). Complex V was so faint that its nature was not clear. Although complex VI was clearly detectable when the probe was incubated with nuclear extract only, moderate bands were also observed in every competitor used. This complex VI might be nonspecific, because there was no difference in the intensity of the bands between each competitor.

Inhibition of Sp1-binding by Sp1-specific chemical inhibitor mithramycin A. Mithramycin A is known to bind to the GC box and inhibit Sp1-binding (6, 21). The effect of mithramycin A on the hPEPT1 promoter activity was investigated with the −401/+60 construct in Caco-2 cells (Fig. 5). Treatment with mithramycin A led to a significant decrease in the promoter activity in a dose-dependent manner.

Transactivation of promoter activity by Sp1 overexpression. Finally, we investigated the effect of Sp1 overexpression on the hPEPT1 promoter activity (Fig. 6). The −401/+60 construct was cotransfected into Caco-2 cells with the CMV-Sp1 expression vector. The luciferase activity showed a dose-dependent increase on cotransfection of CMV-Sp1, providing direct evidence that Sp1 enhanced the promoter activity.

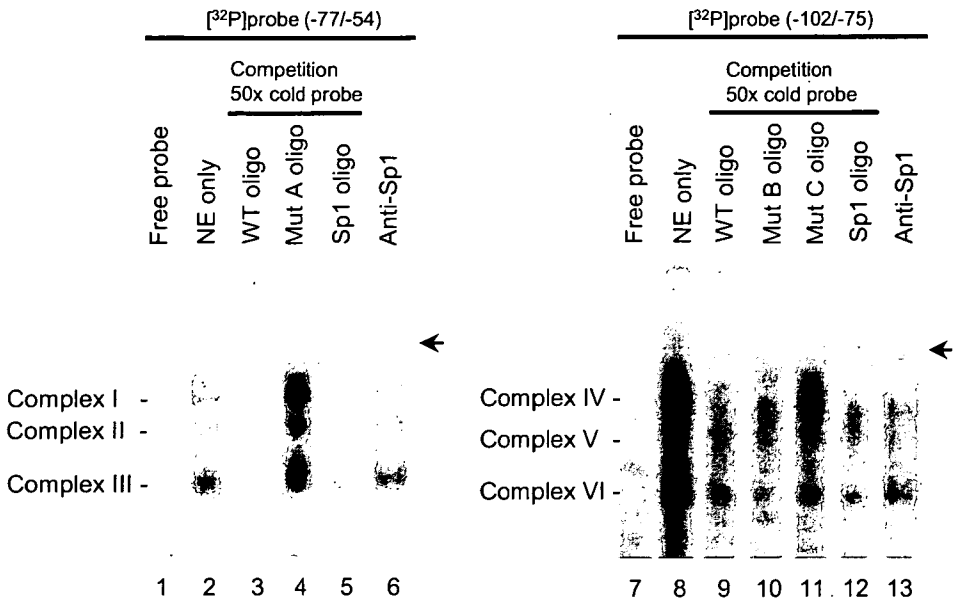

Fig. 4. EMSA of Caco-2 nuclear proteins binding to the probes containing putative Sp1-binding elements. Nuclear extract from Caco-2 cells was incubated with the ^{32}P-labeled oligonucleotide probes (*probe −77/−54* and *probe −102/−75*) alone (*lanes 2* and *8*) or in the presence of excess unlabeled WT oligonucleotide (*lanes 3* and *9*), mutated oligonucleotide (*lanes 4*, *10*, and *11*), Sp1 consensus oligonucleotide (*lanes 5* and *12*), and anti-Sp1 antibody (*lanes 6* and *13*). In *lanes 1* and *7*, nuclear extract was not added. Arrows indicate the supershifted complexes.

DISCUSSION

In the present study, we cloned the 5′-flanking region of the hPEPT1 gene and investigated its transcriptional regulation. When subcloned into a luciferase vector and transfected into Caco-2 cells, the 5′-flanking region showed considerable promoter activity. We used Caco-2 cells because a significant amount of hPEPT1 is expressed constitutively in these cells (2), and the transcription factors and/or cofactors required for the expression exist intrinsically in these cells. In the deletion analysis, the promoter activity was highest with the −401/+60 region, and the minimal promoter was considered to be located in the −172/−35 region. Computational analysis showed the lack of a TATA box and a CAAT box near the transcription start site but the presence of several GC-rich regions. This feature was similar to the mouse PEPT1 promoter, in which a TATA box was not located near the transcription start site, whereas some GC-rich elements were located in the proximal region (9). In such a TATA-less promoter, Sp1 binds to the GC-rich region and this Sp1 site has been shown to be responsible for recruiting TATA-binding protein (20) and fixing the transcription start site (5). Furthermore, the promoter activity is enhanced if multiple Sp1-binding sites exist (14). Thus Sp1 is speculated to play a significant role as a basal

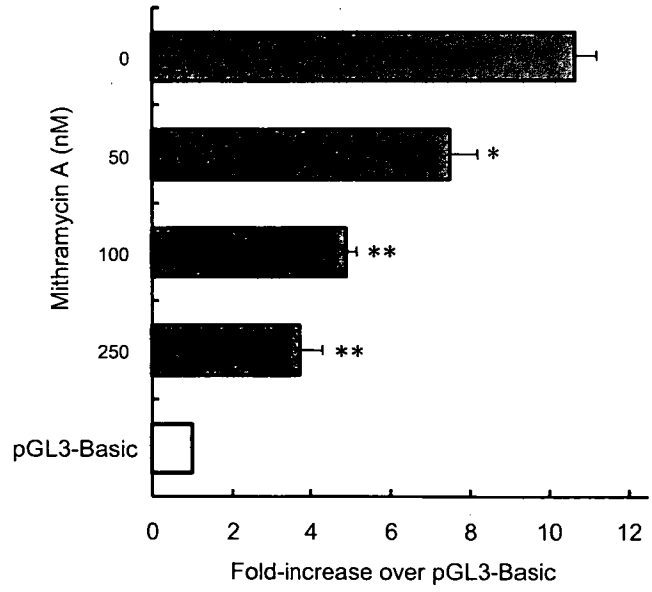

Fig. 5. Inhibition of the hPEPT1 transcriptional activity by mithramycin A. Caco-2 cells were transiently transfected with the −401/+60 construct. Mithramycin A was added to the cells 2 times, just after transfection and after the medium change at 24 h. Firefly luciferase activity was normalized to *Renilla* luciferase activity. Data are reported as the relative fold increase compared with pGL3-Basic vector and represent the means ± SE of 3 replicates. Symbols show significant difference from control (without mithramycin A; $*P < 0.05$ and $**P < 0.01$).

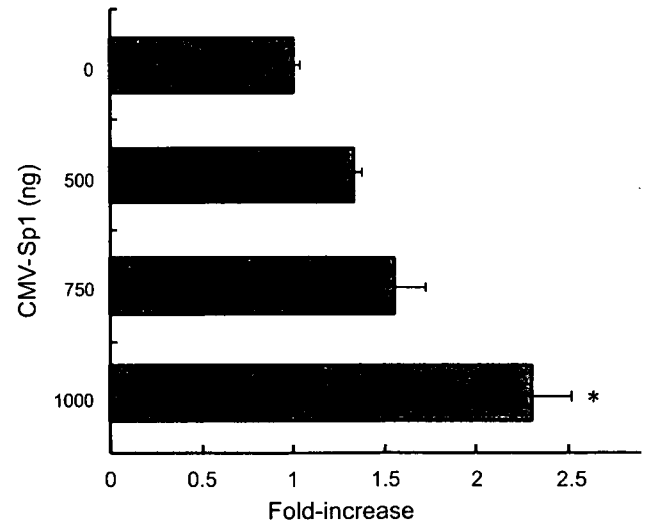

Fig. 6. Effect of Sp1 overexpression on hPEPT1 transcriptional activity. Caco-2 cells were transiently transfected with 250 ng of the −401/+60 construct and 500, 750, and 1,000 ng of the CMV-Sp1 expression vector. The total amount of transfected DNA was kept constant by adding empty vector. Data are reported as the relative fold increase compared with no CMV-Sp1 and represent the means ± SE of 3 replicates. *Significantly different from control (no CMV-Sp1; $P < 0.05$).

transcription factor through these GC-rich sites in the case of the hPEPT1 promoter.

Mutational analysis of these putative Sp1 sites revealed that mutation of Sp-A, Sp-B, or Sp-C site reduced the promoter activity. The EMSA experiment demonstrates that Sp1 binds to Sp-A and Sp-C but not to Sp-B. Collectively, these results suggest that Sp1 binds to both Sp-A and Sp-C sites and significantly contributes to the promoter activity. Although we failed to obtain evidence of the formation of a complex at the Sp-B site in EMSA, some transcription factors may interact with Sp-B and play a role in the basal promoter activity of hPEPT1. The contribution of Sp1 to the promoter activity was confirmed by a different approach, inhibition of Sp1-binding by mithramycin A and the transactivation of the promoter by overexpressed Sp1. Mithramycin A clearly reduced the promoter activity in a dose-dependent manner. Overexpression of Sp1 increased the promoter activity 2.5-fold. These results strongly indicate that Sp1 plays an essential role in the basal transcriptional regulation of hPEPT1. This regulatory mechanism for hPEPT1 was found to be similar to that of other intestinal nutrient transporters, such as Na^+-glucose transporter (SGLT1) (13) and thiamin transporter (16). In both these studies, Sp1 was shown to play a critical role through the GC-box using Caco-2 cells.

Although the present results implicated Sp1 in the basal transcriptional activity of the hPEPT1 promoter, Sp1 is not the only protein acting through GC-rich sites. Other Sp family transcription factors, such as Sp2, Sp3 and Sp4, also interact with GC-rich sites. Among them, Sp3 is ubiquitously expressed in mammalian cells (12) and has a similar affinity for the Sp1-binding site. The present results do not exclude the possibility that Sp3 might also be responsible for the transcriptional regulation of hPEPT1. In addition to Sp family proteins, Krüppel-like factor family proteins (KLFs) also bind with different affinities to GC or GT box (4). Among the Sp family, Sp1, Sp3, and Sp4 have a higher affinity for the GC box than GT box, whereas many of the KLFs bind preferentially to the GT box (4). The Sp-B site has a GT box; thus some KLFs such as GKLF, which is highly expressed in terminally differentiated epithelial cells of the intestine (23), might interact with Sp-B.

hPEPT1 protein is expressed mainly in the small intestine and, to a lesser extent, in the kidney. Although the present study revealed the contribution of Sp1 to the transcriptional regulation of hPEPT1, the mechanism of this tissue-specific expression has not been clarified yet. Computational analysis showed the presence of a binding site for a caudal related homeobox factor, Cdx, within 500 bases upstream of the transcription start site. Cdx-2 is involved in the early differentiation, proliferation, and maintenance of intestinal epithelial cells (25, 27) and in the transcription of intestinal genes, such as the sucrase-isomaltase (26), lactase-phlorizin hydrolase (15), and claudin-2 (22) genes. Although more studies are needed, Cdx-2 may be responsible for the tissue specificity of hPEPT1 expression.

In conclusion, the present results indicate that Sp1 functions as a basal transcriptional regulator of the hPEPT1 gene, and this is the first demonstration to identify the *cis* elements and *trans* factors for the regulation of a human peptide transporter. These findings should serve as a basis for future investigation into the molecular regulation of the transport of nutrient peptides and some pharmaceuticals in the human intestine and other tissues.

ACKNOWLEDGMENTS

We are grateful to Dr. R. Tjian (University of California, Berkeley) for the generous gift of Sp1 expression vector.

GRANTS

This work was supported by the 21st Century COE Program "Knowledge Information Infrastructure for Genome Science," a grant-in-aid for research on advanced medical technology from the Ministry of Health, Labor, and Welfare of Japan, and a grant from the Yamanouchi Foundation for Research on Metabolic Disorders.

REFERENCES

1. **Adibi SA.** Regulation of expression of the intestinal oligopeptide transporter (Pept-1) in health and disease. *Am J Physiol Gastrointest Liver Physiol* 285: G779–G788, 2003.
2. **Ashida K, Katsura T, Motohashi H, Saito H, and Inui K.** Thyroid hormone regulates the activity and expression of the peptide transporter PEPT1 in Caco-2 cells. *Am J Physiol Gastrointest Liver Physiol* 282: G617–G623, 2002.
3. **Berlioz F, Maoret JJ, Paris H, Laburthe M, Farinotti R, and Rozé C.** α_2-Adrenergic receptors stimulate oligopeptide transport in a human intestinal cell line. *J Pharmacol Exp Ther* 294: 466–472, 2000.
4. **Black AR, Black JD, and Azizkhan-Clifford J.** *Sp*1 and krüppel-like factor family of transcription factors in cell growth regulation and cancer. *J Cell Physiol* 188: 143–160, 2001.
5. **Blake MC, Jambou RC, Swick AG, Kahn JW, and Azizkhan JC.** Transcriptional initiation is controlled by upstream GC-box interactions in a TATAA-less promoter. *Mol Cell Biol* 10: 6632–6641, 1990.
6. **Blume SW, Snyder RC, Ray R, Thomas S, Koller CA, and Miller DM.** Mithramycin inhibits SP1 binding and selectively inhibits transcriptional activity of the dihydrofolate reductase gene in vitro and in vivo. *J Clin Invest* 88: 1613–1621, 1991.
7. **Buyse M, Charrier L, Sitaraman S, Gewirtz A, and Merlin D.** Interferon-γ increases hPepT1-mediated uptake of di-tripeptides including the bacterial tripeptide fMLP in polarized intestinal epithelia. *Am J Pathol* 163: 1969–1977, 2003.
8. **Daniel H.** Molecular and integrative physiology of intestinal peptide transport. *Annu Rev Physiol* 66: 361–384, 2004.
9. **Fei YJ, Sugawara M, Liu JC, Li HW, Ganapathy V, Ganapathy ME, and Leibach FH.** cDNA structure, genomic organization, and promoter analysis of the mouse intestinal peptide transporter PEPT1. *Biochim Biophys Acta* 1492: 145–154, 2002.
10. **Fujita T, Majikawa Y, Umehisa S, Okada N, Yamamoto A, Ganapathy V, and Leibach FH.** σ-Receptor ligand-induced up-regulation of the H^+/peptide transporter PEPT1 in the human intestinal cell line Caco-2. *Biochem Biophys Res Commun* 261: 242–246, 1999.
11. **Gangopadhyay A, Thamotharan M, and Adibi SA.** Regulation of oligopeptide transporter (Pept-1) in experimental diabetes. *Am J Physiol Gastrointest Liver Physiol* 283: G133–G138, 2002.
12. **Li L, He S, Sun JM, and Davie JR.** Gene regulation by Sp1 and Sp3. *Biochem Cell Biol* 82: 460–471, 2004.
13. **Martin MG, Wang J, Solorzano-Vargas RS, Lam JT, Turk E, and Wright EM.** Regulation of the human Na^+-glucose cotransporter gene, SGLT1, by HNF-1 and Sp1. *Am J Physiol Gastrointest Liver Physiol* 278: G591–G603, 2000.
14. **Mastrangelo IA, Courey AJ, Wall JS, Jackson SP, and Hough PVC.** DNA looping and Sp1 multimer links: a mechanism for transcriptional synergism and enhancement. *Proc Natl Acad Sci USA* 88: 5670–5674, 1991.
15. **Mitchelmore C, Troelsen JT, Spodsberg N, Sjostrom H, and Noren O.** Interaction between the homeodomain proteins Cdx2 and HNF1alpha mediates expression of the lactase-phlorizin hydrolase gene. *Biochem J* 346: 529–535, 2000.
16. **Nabokina SM and Said HM.** Characterization of the 5′-regulatory region of the human thiamin transporter SLC19A3: in vitro and in vivo studies. *Am J Physiol Gastrointest Liver Physiol* 287: G822–G829, 2004.
17. **Naruhashi K, Sai Y, Tamai I, Suzuki N, and Tsuji A.** Pept1 mRNA expression is induced by starvation and its level correlates with absorptive

transport of cefadroxil longitudinally in the rat intestine. *Pharm Res* 19: 1417–1423, 2002.

18. **Nielsen CU, Amstrup J, Steffansen B, Frokjaer S, and Brodin B.** Epidermal growth factor inhibits glycylsarcosine transport and hPepT1 expression in a human intestinal cell line. *Am J Physiol Gastrointest Liver Physiol* 281: G191–G199, 2001.
19. **Pan X, Terada T, Irie M, Saito H, and Inui K.** Diurnal rhythm of H^+-peptide cotransporter in the rat small intestine. *Am J Physiol Gastrointest Liver Physiol* 283: G57–G64, 2002.
20. **Pugh BF and Tjian R.** Transcription from a TATA-less promoter requires a multisubunit TFIID complex. *Genes Dev* 5: 1935–1945, 1991.
21. **Ray R, Snyder RC, Thomas S, Koller CA, and Miller DM.** Mithramycin blocks protein binding and function of the SV40 early promoter. *J Clin Invest* 83: 2003–2007, 1989.
22. **Sakaguchi T, Gu X, Golden HM, Suh E, Rhoads DB, and Reinecker HC.** Cloning of the human claudin-2 5′-flanking region revealed a TATA-less promoter with conserved binding sites in mouse and human for caudal-related homeodomain proteins and hepatocyte nuclear factor-1 alpha. *J Biol Chem* 277: 21361–21370, 2002.
23. **Shields JM, Christy RJ, and Yang VW.** Identification and characterization of a gene encoding a gut-enriched Krüppel-like factor expressed during growth arrest. *J Biol Chem* 271: 20009–20017, 1996.
24. **Shiraga T, Miyamoto K, Tanaka H, Yamamoto H, Taketani Y, Morita K, Tamai I, Tsuji A, and Takeda E.** Cellular and molecular mechanisms of dietary regulation on rat intestinal H^+/peptide transporter PepT1. *Gastroenterology* 116: 354–362, 1999.
25. **Silberg DG, Swain GP, Suh ER, and Traber PG.** Cdx1 and Cdx2 expression during intestinal development. *Gastroenterology* 119: 961–971, 2000.
26. **Suh E, Chen L, Taylor J, and Traber PG.** A homeodomain protein related to caudal regulates intestine-specific gene transcription. *Mol Cell Biol* 14: 7340–7351, 1994.
27. **Suh E and Traber PG.** An intestine-specific homeobox gene regulates proliferation and differentiation. *Mol Cell Biol* 16: 619–625, 1996.
28. **Terada T and Inui K.** Peptide transporters: structure, function, regulation and application for drug delivery. *Curr Drug Metabol* 5: 85–94, 2004.
29. **Urtti A, Johns SJ, and Sadee W.** Genomic structure of proton-coupled oligopeptide transporter *hPEPT1* and pH sensing regulatory splice variant. *AAPS Pharm Sci* 3: E6, 2001.

Available online at www.sciencedirect.com
SCIENCE DIRECT
Biochemical Pharmacology 70 (2005) 1104–1113
Biochemical Pharmacology
www.elsevier.com/locate/biochempharm

Human organic anion transporter hOAT3 is a potent transporter of cephalosporin antibiotics, in comparison with hOAT1

Harumasa Ueo, Hideyuki Motohashi, Toshiya Katsura, Ken-ichi Inui *

Department of Pharmacy, Kyoto University Hospital, Faculty of Medicine, Kyoto University, Kyoto 606-8507, Japan

Received 7 June 2005; accepted 29 June 2005

Abstract

We examined the substrate specificity of human organic anion transporter (hOAT) 1 and hOAT3 for various cephalosporin antibiotics, cephaloridine, cefdinir, cefotiam, ceftibuten, cefaclor, ceftizoxime, cefoselis and cefazolin by using HEK293 cells stably transfected with hOAT1 or hOAT3 cDNA (HEK-hOAT1, HEK-hOAT3). Additionally, we examined the uptake of various compounds by these transfectants. The mRNA level of hOAT3 in HEK-hOAT3 was about three-fold that of hOAT1 in HEK-hOAT1. Functional expression of hOAT1 and hOAT3 was confirmed by the uptake of *p*-[^{14}C]aminohippurate and [^{3}H]estrone sulfate, respectively. *p*-[^{14}C]Aminohippurate, [^{3}H]estrone sulfate, [^{14}C]captopril, [^{3}H]methotrexate, [^{3}H]ochratoxin A, [^{3}H]leucovorin and [^{3}H]cimetidine were shown to be substrates for hOAT1 and hOAT3, and [^{3}H]dehydroepiandrosterone sulfate was shown to be a substrate for hOAT3. All cephalosporin anitibiotics tested were shown to inhibit the uptake of *p*-[^{14}C]aminohippurate and [^{3}H]estrone sulfate via hOAT1 and hOAT3, respectively, in a dose-dependent manner, and the IC_{50} values of these antibiotics, except for cefaclor, for the hOAT1-mediated uptake of *p*-[^{14}C]aminohippurate were within four-fold of those for the hOAT3-mediated uptake of [^{3}H]estrone sulfate. The uptake of cephaloridine, cefdinir and cefotiam by HEK-hOAT3 was 35–50-fold greater than that by control cells. Moreover, the accumulation of the other cephalolsporin antibiotics was significantly greater in HEK-hOAT3 than in control cells. In contrast, the uptake of these antibiotics by HEK-hOAT1 was within two-fold of that by control cells. In conclusion, hOAT3 plays a more important role than hOAT1 in the renal secretion of cephalosporin antibiotics.
© 2005 Elsevier Inc. All rights reserved.

Keywords: Organic anion transporter; Cephalosporin antibiotics; *p*-Aminohippurate; Estrone sulfate; Renal secretion; Transport

1. Introduction

In the kidney, organic anion transporters, which are expressed in the apical and basolateral membranes of tubular epithelial cells, are responsible for tubular secretion of organic anions including drugs, toxins and endogenous compounds [1–3]. Cloned human organic anion transporters (hOATs) have been shown to transport clinically important drugs, such as antiviral agents [4], nonsteroidal anti-inflammatory drugs (NSAIDs) [5] and diuretics [6]. We previously reported that mRNA levels of hOAT1 and hOAT3 were much higher than those of other organic ion transporters in the human kidney cortex, and that hOAT1 and hOAT3 were localized to the basolateral membrane of the proximal tubular cells [7]. These results suggest that hOAT1 and hOAT3 play important roles in the tubular uptake of various drugs from the circulation. Therefore, for elucidation of the mechanism behind the renal elimination of various drugs, it is important to characterize the substrate specificities of these transporters.

Most cephalosporin antibiotics are excreted into urine in nonmetabolized forms, and renal tubular secretion appears to be an important pathway for their renal clearance [8]. Several in vivo and in vitro studies have tried to elucidate the transport mechanisms of cephalosporins in the kidney [9–11]. From these findings, it was suggested that OATs would be involved in the renal secretion of cephalosporins. Actually, rat OAT1 transported cephalosporins [12].

Abbreviations: hOAT, human organic anion transporter; rOAT, rat organic anion transporter

* Corresponding author. Tel.: +81 75 751 3577; fax: +81 75 751 4207.
E-mail address: inui@kuhp.kyoto-u.ac.jp (K.-i. Inui).

0006-2952/$ – see front matter © 2005 Elsevier Inc. All rights reserved.
doi:10.1016/j.bcp.2005.06.024

With regard to human OATs, Takeda et al. [13] reported that cephalosporin antibiotics interacted with hOATs. However, it has not been clarified whether hOATs are responsible for the tubular secretion of antibiotics. In our previous study, it was recognized that hOAT3 mediated the transport of cefazolin [14]. Moreover, renal excretion of cefazolin was significantly correlated with hOAT3 mRNA levels in patients with renal diseases, suggesting that hOAT3 plays an important role in the secretion of cefazolin in such patients [14]. It has remained to be elucidated whether hOAT1 or hOAT3 transports other cephalosporins.

In this study, we examined the transport of various cephalosporin antibiotics by hOAT1 and hOAT3 to characterize the substrate specificity of these transporters.

2. Materials and methods

2.1. Materials

p-[Glycyl-1-^{14}C]aminohippurate (1.9 GBq/mmol) and [1,2,6,7-^{3}H(*N*)]dehydroepiandrosterone sulfate, sodium salt (2.2 TBq/mmol) were obtained from NEN™ Life Science Products Inc. (Boston, MA). [6,7-^{3}H(*N*)]estrone sulfate, ammonium salt (2.1 TBq/mmol) was from Perkin-Elmer Life Sciences Inc. (Boston, MA). [^{14}C]captopril (115 MBq/mmol) was from Sankyo Co. (Tokyo, Japan). [3′,5′,7′-^{3}H(*N*)]methotrexate, disodium salt (851 GBq/mmol), [^{3}H(G)]ochratoxin A (666 GBq/mmol) and [3′,5′,7′,9′-^{3}H] (6*S*)-leucovorin, diammonium salt (962 GBq/mmol) were from Moravek Biochemicals Inc. (Brea, CA). [*N*-Methyl-^{3}H]Cimetidine (451 GBq/mmol) was from Amersham Biosciences (Uppsala, Sweden). Cefaclor, cephaloridine and ceftibuten (Shionogi Co., Osaka, Japan), cefdinir, ceftizoxime, cefoselis and cefazolin (Fujisawa Pharmaceutical Co., Osaka, Japan) and cefotiam (Takeda Chemical Industries, Osaka, Japan) were gifts from the respective suppliers. All other chemicals used were of the highest purity available.

2.2. Cell culture and transfection

HEK 293 cells (American Type Culture Collection CRL-1573), a transformed cell line derived from human embryonic kidney, were cultured in complete medium consisting of Medium 199 (Invitrogen, Carlsbad, CA) with 10% fetal bovine serum (Thermo. Electron Co., Waltham, MA) (Invitrogen) in an atmosphere of 5% CO_2, 95% air at 37 °C. hOAT1 and hOAT3 cDNAs were subcloned into pBK-CMV plasmid vector (Stratagene, La Jolla, CA). HEK 293 cells were transfected with hOAT1 cDNA, hOAT3 cDNA or empty vector using LipofectAMINE 2000 (Invitrogen) according to the manufacturer's instructions. G418 (Nacalai Tesque, Kyoto, Japan) (0.5 mg/ml)—resistant cells were removed. Cells expressing hOAT1 (HEK-hOAT1) were selected by measuring *p*-[^{14}C]aminohippurate uptake, and cells expressing hOAT3 (HEK-hOAT3) were selected by measuring [^{3}H]estrone sulfate uptake. Cells transfected with empty vector (HEK-pBK) were used as control cells. These transfectants were maintained in complete medium with G418 (0.5 mg/ml).

2.3. Quantification of mRNA expression of hOATs in HEK-hOAT1 and HEK-hOAT3

Total RNA was extracted from HEK-hOAT1 or HEK-hOAT3 using an RNeasy mini kit (Qiagen, Hilden, Germany) according to the manufacturer's instructions and reverse-transcribed using SuperScriptsTMII RT (Invitrogen, Grand Island, NY). For quantification of the amounts of hOAT1 and hOAT3 mRNA, the real-time PCR method was carried out using the ABI PRISM 7700 sequence detector (Applied Biosystems, Foster, CA). Glyceraldehyde-3-phosphate dehydrogenase (GAPDH) mRNA was also quantified as an internal control with GAPDH Control Reagent (Applied Biosystems).

2.4. Uptake of various compounds by HEK-hOAT1 or HEK-hOAT3

Uptake experiments were performed as described previously [15] with some modifications. HEK-hOAT1 and HEK-hOAT3 were seeded on poly-D-lysine-coated 24-well plates at a density of 2×10^5 cells/well for the uptake of *p*-[^{14}C]aminohippurate, [^{3}H]estrone sulfate, [^{14}C]captopril, [^{3}H]methotrexate, [^{3}H]ochratoxin A, [^{3}H]leucovorin, [^{3}H]cimetidine and [^{3}H]dehydroepiandrosterone sulfate. At 48 h after seeding, the uptake of these compounds by HEK-hOAT1 or HEK-hOAT3 was examined. The composition of the incubation medium was as follows (in mM): 145 NaCl, 3 KCl, 1 $CaCl_2$, 0.5 $MgCl_2$, 5 D-glucose and 5 HEPES (pH 7.4). The cells were preincubated with 0.2 ml of the incubation medium for 10 min at 37 °C. After the preincubation, the medium was replaced with 0.2 ml of incubation medium containing each anionic compound. At the end of the incubation period, the medium was aspirated, and then cells were washed two times with 1 ml of ice-cold incubation medium. The cells were lysed in 0.25 ml of 0.5N NaOH solution, and the radioactivity in aliquots was determined in 3 ml of ACSII (Amersham International, Buckingham shire, UK). The protein contents of the solubilized cells were determined by the method of Bradford [16] using the Bio-Rad Protein Assay kit (Bio-Rad, Hercules, CA) with bovine γ-globulin as a standard.

2.5. Uptake of cephalosporin antibiotics by HEK 293 cells stably expressing hOAT1 or hOAT3

For the experiments on the uptake of cephalosporin antibiotics, HEK-hOAT1 and HEK-hOAT3 were seeded

on 6-cm poly-D-lysine-coated dishes at a density of 2×10^6 cells/dish. At 48 h after seeding, the uptake of cephalosporin antibiotics was examined. The cells were preincubated with 2 ml of the incubation medium for 10 min at 37 °C. After this preincubation, the medium was replaced with 2 ml of incubation medium containing various cephalosporin antibiotics. At the end of the incubation period, the medium was aspirated, and then cells were washed three times with 5 ml of ice-cold incubation medium. To measure the accumulation of cephalosporin antibiotics, the cells were scraped and homogenized with 1 ml of water. Protein levels were determined with 5 μl of the homogenate. For the determination of cephalosporin antibiotics, to 0.9 ml of the homogenate, 100 μl of water and 20 μl of phosphoric acid were added and mixed for 30 s, then 1.0 ml of the sample was loaded onto an Oasis HLB cartridge (Waters Corporation, Milford, MA) preconditioned with 1 ml each of methanol and water. The column was washed with 1 ml of 5% methanol and cephalosporin antibiotic was eluted from the column with 1 ml of methanol. The eluate was evaporated to dry at 45–50 °C and resuspended in 200 μl of mobile phase buffer. The solution was filtered through a 0.45-μm polyvinylidene fluoride filter. The concentration of cephalosporin antibiotic was measured by use of a high performance liquid chromatograph (LC-10AT, LC-10AD, Shimadzu Co., Kyoto, Japan) equipped with a UV spectrophotometric detector (SPD-10AV, SPD-10A, Shimadzu) under the following conditions: column, Zorbax ODS column 4.6 mm inside diameter × 250 mm (Du Pont, Wilmington, DE); mobile phase, 30 mM citric acid buffer in methanol at 85:15 for cefdinir, ceftibuten, cefaclor, ceftizoxime and cefoselis, 30 mM phosphate buffer (pH 5.2) in methanol at 83:17 for cephaloridine and cefazolin, 30 mM phosphate buffer (pH 6.5) in methanol at 78:22 for cefotiam; flow rate, 0.8 ml/min; wave length, 254 nm for cephaloridine, cefotiam, ceftibuten, ceftizoxime and cefoselis, 288 nm for cefdinir, 266 nm for cefaclor, 272 nm for cefazolin; injection volume, 50 μl; temperature, 40 °C.

2.6. Statistical analysis

Data were analysed statistically using nonpaired *t*-tests.

3. Results

3.1. Construction of HEK-hOAT1 and HEK-hOAT3

In a previous study, we performed the characterization of the uptake of *p*-[^{14}C]aminohippurate and [^{3}H]estrone sulfate in HEK 293 cells transfected with hOAT1 and hOAT3 cDNA, respectively, using transient expression systems [14]. In this study, we constructed HEK 293 cells stably expressing hOAT1 or hOAT3. First, mRNA levels of hOAT1 and hOAT3 were investigated by real-time PCR. The mRNA level of hOAT1 in HEK-hOAT1 was quantified to be 64.9 amol/μg total RNA, and that of hOAT3 in HEK-hOAT3 was 225.6 amol/μg total RNA. The functional expression of hOAT1 and hOAT3 was assessed by the uptake of *p*-[^{14}C]aminohippurate and [^{3}H]estrone sulfate by HEK-hOAT1 and HEK-hOAT3, respectively. Fig. 1 shows that HEK-hOAT1 and HEK-hOAT3 exhibited time-dependent uptake of *p*-[^{14}C]aminohippurate and [^{3}H]estrone sulfate, respectively. As shown in Fig. 2, a concentration-dependent uptake of *p*-[^{14}C]aminohippurate and [^{3}H]estrone sulfate by HEK-hOAT1 and HEK-hOAT3, respectively, was observed. Using a nonlinear least squares regression analysis, kinetic parameters were calculated according to the Michaelis-Menten equation in three separate experiments. Apparent Michaelis-Menten constants (K_m) for the uptake of *p*-[^{14}C]aminohippurate by HEK-hOAT1 and of [^{3}H]estrone sulfate by HEK-hOAT3 were

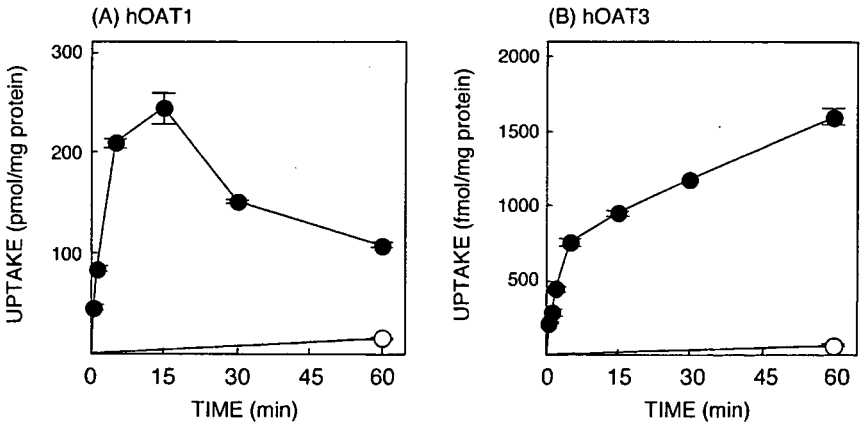

Fig. 1. Time course of *p*-[^{14}C]aminohippurate (A) and [^{3}H]estrone sulfate (B) accumulation in HEK-hOAT1 and HEK-hOAT3, respectively. (A) *p*-[^{14}C]Aminohippurate accumulation in HEK-pBK (○) or HEK-hOAT1 (●). The cells were incubated with 5 μM *p*-[^{14}C]aminohippurate for the periods indicated at 37 °C. (B) [^{3}H]Estrone sulfate accumulation in HEK-pBK (○) or HEK-hOAT3 (●). The cells were incubated with 20 nM [^{3}H]estrone sulfate for the periods indicated at 37 °C. After the incubation, the radioactivity of solubilized cells was measured. Each point represents the mean ± S.E. of three monolayers from a typical experiment.

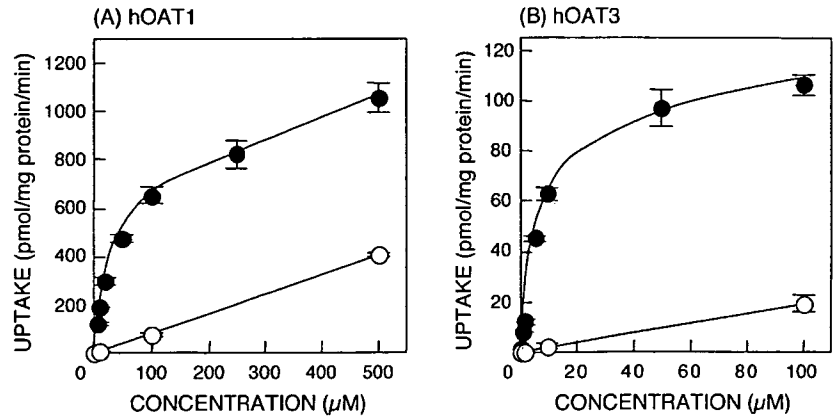

Fig. 2. Concentration dependence of *p*-[^{14}C]aminohippurate (A) and [^{3}H]estrone sulfate (B) accumulation in HEK-hOAT1 and HEK-hOAT3, respectively. HEK-hOAT1 and HEK-hOAT3 were incubated with various concentrations of *p*-[^{14}C]aminohippurate or [^{3}H]estrone sulfate in the absence (●) or presence (○) of unlabeled 5 mM *p*-aminohippurate (A) or 1 mM estrone sulfate (B) for 1 min at 37 °C. After the incubation, the radioactivity of solubilized cells was measured. Each point represents the mean ± S.E. of three monolayers from a typical experiment.

28.0 ± 1.9 and 6.3 ± 2.2 μM (n = 3, mean ± S.E.), respectively, which were consistent with previous reports [17–19]. Maximal uptake rate (V_{max}) values for HEK-hOAT1 and HEK-hOAT3 were 553.2 ± 70.9 and 102.7 ± 19.7 pmol/mg protein/min (n = 3, mean ± S.E.), S.E.), respectively.

In addition, we measured the uptake of various compounds by these transfectants. Results of these uptake experiments are shown in Fig. 3. A remarkable increase in the uptake of *p*-[^{14}C]aminohippurate, [^{14}C]captopril, [^{3}H]ochratoxin A and [^{3}H]leucovorin, and slight increase (within two-fold) in the uptake of [^{3}H]estrone sulfate, [^{3}H]methotrexate and [^{3}H]cimetidine were observed in HEK-hOAT1 compared to control cells. A remarkable increase in the uptake of *p*-[^{14}C]aminohippurate, [^{3}H]estrone sulfate, [^{14}C]captopril, [^{3}H]methotrexate, [^{3}H]ochratoxin A, [^{3}H]leucovorin, [^{3}H]cimetidine and [^{3}H]dehydroepiandrosterone sulfate was observed in HEK-hOAT3 compared to control cells.

3.2. Inhibitory effects of cephalosporin antibiotics on hOAT1 and hOAT3

To determine the affinity of cephalosporins for hOAT1 and hOAT3, we examined the inhibitory effects of these drugs on the uptake of *p*-[^{14}C]aminohippurate and [^{3}H]estrone sulfate by HEK-hOAT1 and HEK-hOAT3, respectively. As shown in Fig. 4, cephalosporin anitibiotics inhibited the uptake of organic anions by HEK-hOAT1 and HEK-hOAT3 in a dose-dependent manner. The IC_{50} values were estimated by nonlinear regression analysis of the competition curves with a one-compartment model with the following equation: $V = 100 \times IC_{50}/(IC_{50} + [I]) + A$, where V the uptake amount (% of control), [I] the concentration of cephalosporin antibiotic and A is the nonspecific organic anion uptake (% of control). The findings are summarized in Table 1.

3.3. Characterization of the uptake of cephalosporin antibiotics by hOAT1 and hOAT3

To investigate whether hOAT1 and hOAT3 transport cephalosporin antibiotics, we measured the accumulations of these drugs in HEK-hOAT1 and HEK-hOAT3. As shown in Fig. 5, the uptake of cephaloridine, cefdinir and cefotiam by HEK-hOAT3 was 35–50-fold higher than that by control cells. Moreover, the accumulation of ceftibuten, cefaclor, ceftizoxime, cefoselis and cefazolin was significantly greater in HEK-hOAT3 than in control cells. Those cephalosporin antibiotics whose accumulation was significantly greater in HEK-hOAT1 than control cells were cephaloridine, cefdinir, ceftibuten and ceftizoxime. The uptake of these antibiotics by HEK-hOAT1 was within two-fold of that by control cells.

Fig. 6 shows the time course of the uptake of cephaloridine, cefotiam or cefazolin by HEK-hOAT1 or HEK-hOAT3. The accumulation of cephaloridine, cefotiam and cefazolin in HEK-hOAT3 increased markedly in a time-dependent manner. The accumulation of these antibiotics in HEK-hOAT1 was comparable to that in control cells.

Table 1
The IC_{50} values of various cephalosporin antibiotics for the uptake of *p*-aminohippurate and estrone sulfate by hOAT1 and hOAT3, respectively

Cephalosporin	IC_{50} (μM)	
	hOAT1	hOAT3
Cephaloridine	2470.0 ± 339.3	626.4 ± 66.7
Cefdinir	691.8 ± 222.9	271.5 ± 46.5
Cefotiam	639.7 ± 63.0	212.6 ± 26.9
Ceftibuten	563.1 ± 50.1	247.3 ± 74.0
Cefaclor	1095.6 ± 95.9	120.2 ± 7.2
Ceftizoxime	3598.6 ± 368.6	956.7 ± 29.7
Cefoselis	2600.5 ± 439.3	2925.1 ± 27.1
Cefazolin[a]	100.6 ± 25.3	116.6 ± 13.0

The values represent the means ± S.E. of three separate experiments.
[a] Values are from Ref. [14].

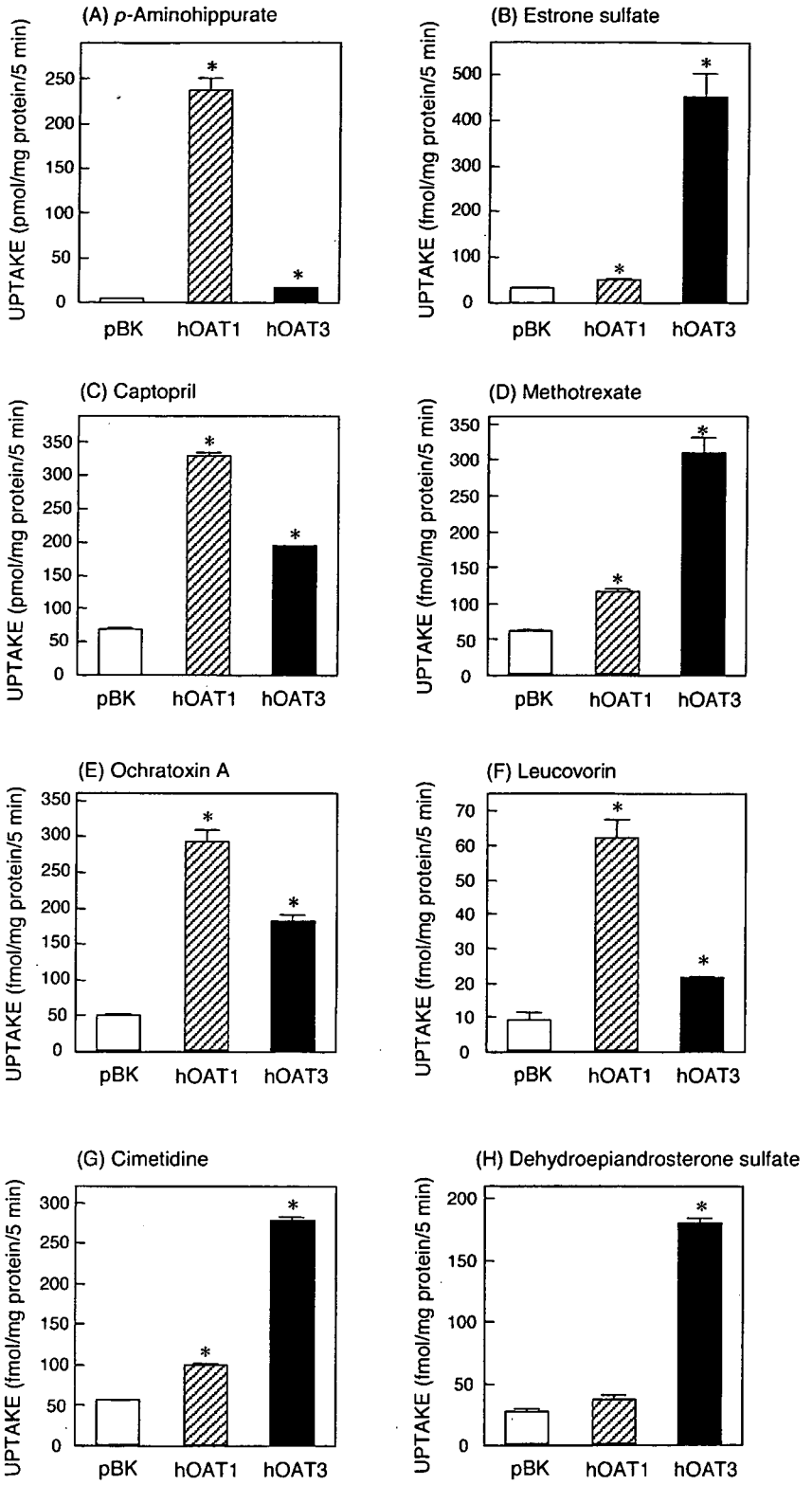

Fig. 3. Uptake of various anionic compounds by HEK-hOAT1 or HEK-hOAT3. HEK-pBK, HEK-hOAT1 and HEK-hOAT3 were incubated with 5 μM *p*-[^{14}C]aminohippurate (A), 20 nM [^{3}H]estrone sulfate (B), 160 μM [^{14}C]captopril (C), 40 nM [^{3}H]methotrexate (D), 20 nM [^{3}H]ochratoxin A (E), 40 nM [^{3}H]leucovorin (F), 80 nM [^{3}H]cimetidine (G) or 20 nM [^{3}H]dehydroepiandrosterone sulfate (H) for 5 min at 37 °C. After the incubation, the radioactivity of solubilized cells was measured. Each column represents the mean ± S.E. of three monolayers from a typical experiment. $^{*}p < 0.05$, significant differences from control.

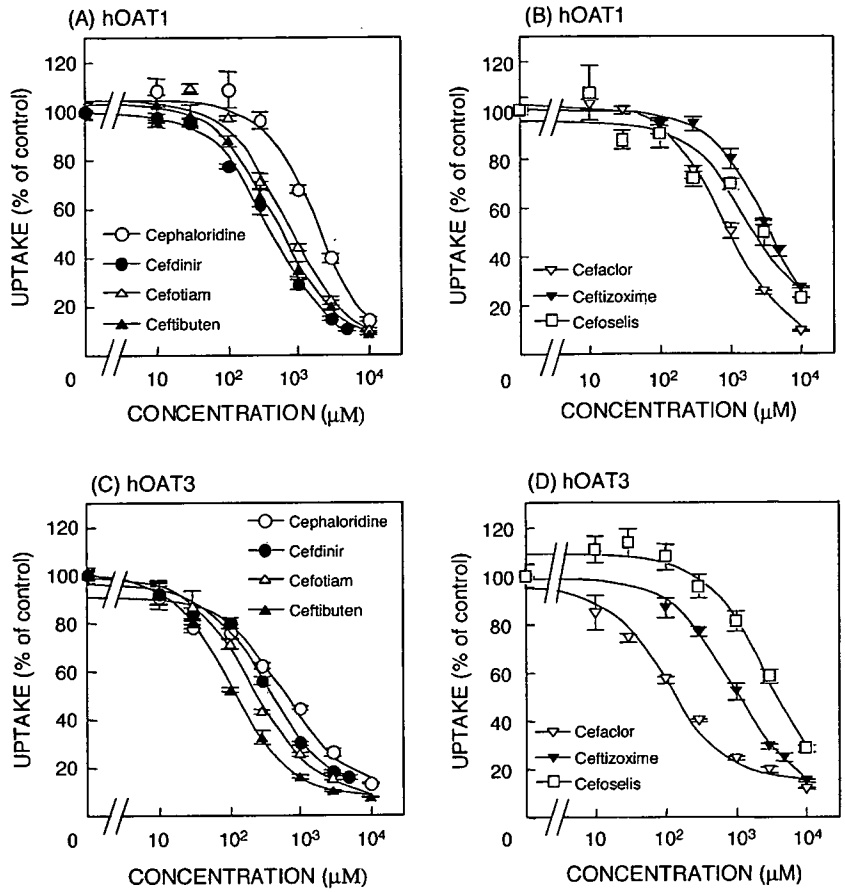

Fig. 4. Effects of cephalosporin antibiotics on the uptake of *p*-[^{14}C]aminohippurate (A and B) and [^{3}H]estrone sulfate (C and D) by HEK-hOAT1 and HEK-hOAT3, repectively. HEK-hOAT1 and HEK-hOAT3 was incubated with 5 μM *p*-[^{14}C]aminohippurate (A and B) and 20 nM [^{3}H]estrone sulfate (C and D), respectively, for 1 min at 37 °C in the presence of various concentrations of cephaloridine (○), cefdinir (●), cefotiam (△), ceftibuten (▲), cefaclor (▽), ceftizoxime (▼) or cefoselis (□). After the incubation, the radioactivity of solubilized cells was measured. Each point represents the mean ± S.E. of three monolayers from a typical experiment.

4. Discussion

Renal organic anion transporters, hOAT1 and hOAT3, mediate the basolateral uptake of various drugs in proximal tubules. In our previous studies, Uwai et al. [12] reported that rOAT1 transported cephalosporin antibiotics, cefazolin, cefotiam and cefalexin, and Sakurai et al. [14] reported that hOAT3 plays an important role in the renal secretion of cefazolin in patients with renal diseases. The present study examined the transport of various cephalosporin antibiotics via hOAT1 and hOAT3. In this study, for all cephalosporin antibiotics tested, particularly, cephaloridine, cefdinir and cefotiam, the uptake by HEK-hOAT3 was greater than that by HEK-hOAT1. The mRNA level of hOAT3 in HEK-hOAT3 was about three-fold higher than that of hOAT1 in HEK-hOAT1, and we have previously reported that the level of hOAT3 mRNA is about three-fold higher than that of hOAT1 mRNA in human kidney [7]. Therefore, we suggest that the uptake by HEK-hOAT1 and HEK-hOAT3 reflects to some extent the basolateral uptake via hOAT1 and hOAT3 in renal epithelial cells. The present results showed that hOAT3 plays a major role in the basolateral uptake of various cephalosporin antibiotics, as well as cefazolin [14], into epithelial cells from the blood.

We examined the transport of various compounds via hOAT1 and hOAT3. It has been suggested that hOAT3 can mediate the transport of organic anions with bulky side groups, compared with hOAT1 [18], and in the current study, the remarkable increase in the uptake of [^{3}H]estrone sulfate and [^{3}H]dehydroepiandrosterone sulfate was observed in HEK-hOAT3 compared to control cells, while little or no increase was observed in HEK-hOAT1. Nevertheless, the difference in substrate specificity between hOAT1 and hOAT3 remains to be properly elucidated. We previously reported that hOAT1 mRNA levels are significantly lower in the kidneys of patients with renal diseases than in the normal kidney cortex, whereas hOAT3 mRNA levels are not significantly reduced, and suggested that each transporter undergoes a different effect in the impaired kidney [14]. By combining information about the alteration in the expression level and substrate specificity of a transporter, we could at least in part contribute to establishment of the administration schedule in cases of renal disease.

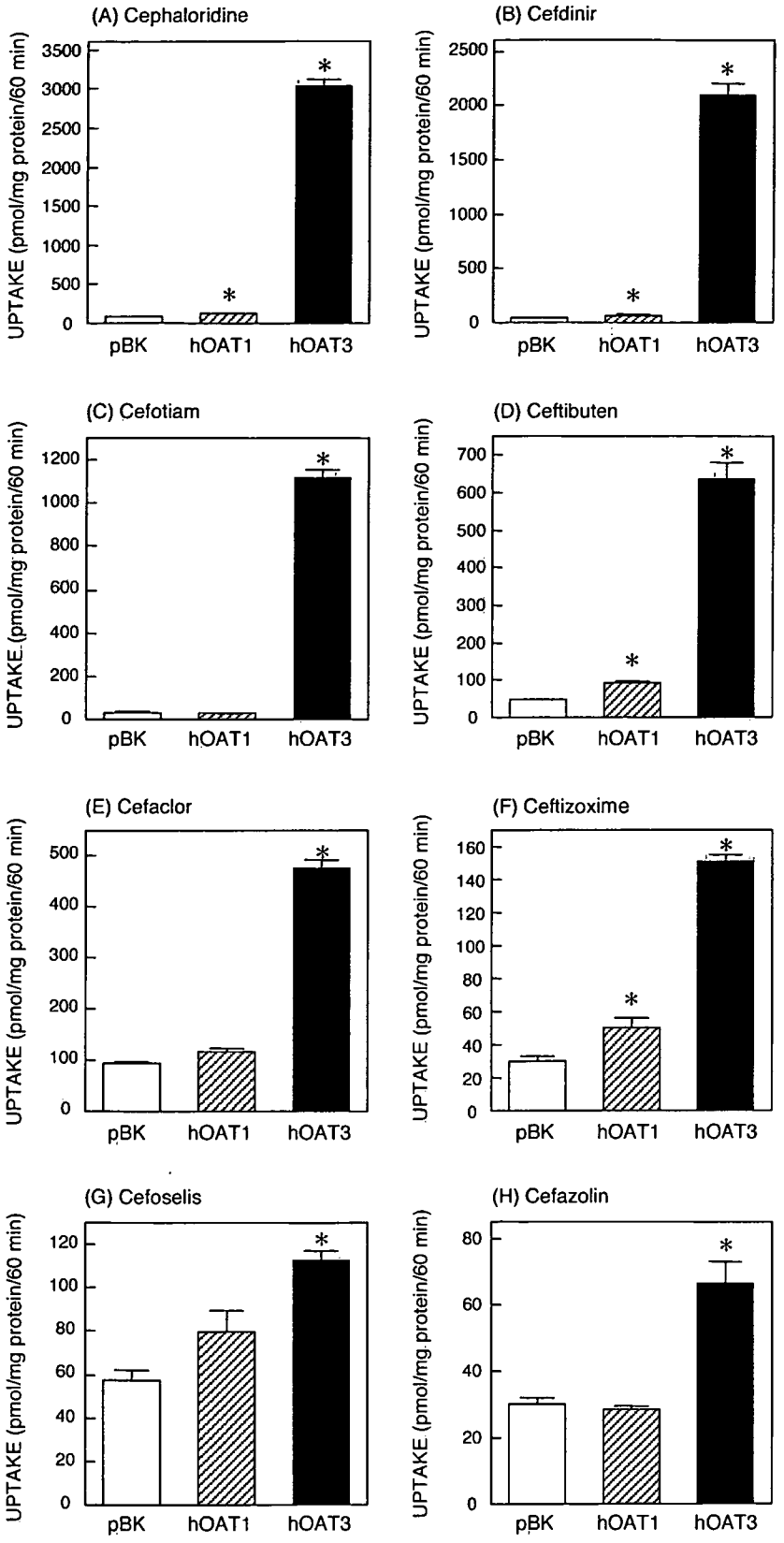

Fig. 5. Uptake of cephalosporin antibiotics by HEK-hOAT1 and HEK-hOAT3. HEK-pBK, HEK-hOAT1 and HEK-hOAT3 were incubated for 60 min at 37 °C with 500 μM cephaloridine (A), cefdinir (B), cefotiam (C), ceftibuten (D), cefaclor (E), ceftizoxime (F), cefoselis (G) or cefazolin (H). After the incubation, the accumulation of these antibiotics in the cells was measured by use of a high performance liquid chromatograph. Each column represents the mean ± S.E. of three monolayers from a typical experiment. $^{*}p < 0.05$, significant differences from control.

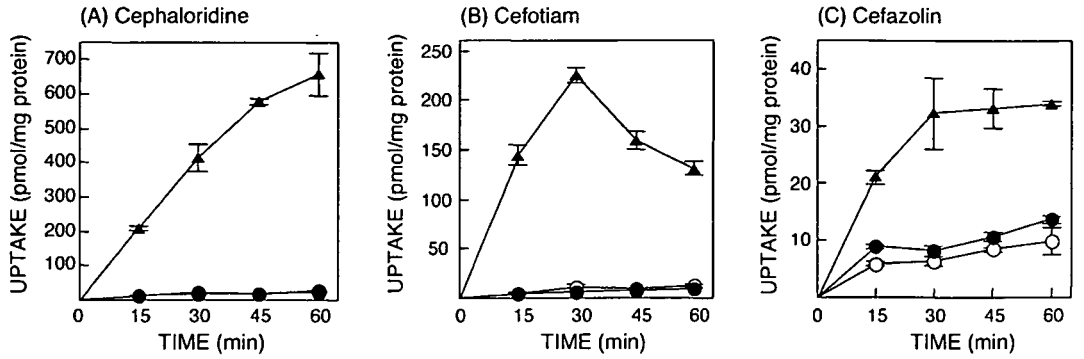

Fig. 6. Time course of cephaloridine (A), cefotiam (B) and cefazolin (C) accumulation in HEK-hOAT1 and HEK-hOAT3. HEK-pBK (○), HEK-hOAT1 (●) and HEK-hOAT3 (▲) were incubated for the indicated periods at 37 °C with 100 μM cephaloridine (A), 200 μM cefotiam (B) or 200 μM cefazolin (C). After the incubation, the accumulation of these antibiotics in the cells was measured by use of a high performance liquid chromatograph. Each point represents the mean ± S.E. of three monolayers from a typical experiment.

Uwai et al. [20] reported that probenecid markedly inhibited the transport of *p*-aminohippurate via rOAT1, although was not transported via rOAT1. Zhang et al. [21] showed that HIV protease inhibitors including indinavir, nelfinavir, ritonavir and saquinavir are potent inhibitors of hOCT1; however, they are poor substrates for hOCT1-mediated transport. In the current study, the IC_{50} values of cephaloridine, cefdinir and cefotiam for the hOAT1-mediated uptake of *p*-[^{14}C]aminohippurate were within four-fold of those for the hOAT3-mediated uptake of [^{3}H]estrone sulfate. On the other hand, the uptake of these antibiotics by HEK-hOAT3 (35–50-fold higher than that by control cells) was remarkably greater than that by HEK-hOAT1 (within 1.6-fold of that by control cells). In addition, although the IC_{50} value of cephaloridine was six-fold higher than that of cefazolin for hOAT3-mediated organic anion uptake, cephaloridine uptake was 46-fold higher than cefazolin uptake in HEK-hOAT3. The results suggested that these marked differences in transport activity are due to the efficacy of the translocation process. These previous findings and the current study have indicated that it is necessary to investigate not only substrate affinity but also substrate transport when characterizing the substrate specificity of a transporter.

Cephaloridine produces acute renal failure in humans and animals [22]. In the kidney, cephaloridine is rapidly transported into the epithelial cells, but undergoes minimal subsequent movement into the lumen [23], and the accumulation of drug in the tubular cells attributable to this process plays a role in the mechanism of renal failure [24]. It has been reported that rOAT1 and rOAT3 are, at least in part, responsible for the basolateral uptake of cephaloridine and therefore cephaloridine-induced renal failure [25,26]. In a previous study, the K_i values of cephaloridine for the rOAT1 and rOAT3-mediated uptake of organic anions were similar (1.32 mM for rOAT1 and 1.14 mM for rOAT3) and it was suggested that both rOAT1 and rOAT3 participate in the transport of cephaloridine and in cephaloridine-induced renal failure, although the uptake of cephaloridine by these transporters was not compared [26]. In the current study, the uptake of cephaloridine by HEK-hOAT3 was remarkably higher than that by HEK-hOAT1, demonstrating that hOAT3 plays a more important role in cephaloridine-induced renal failure than hOAT1.

Lu et al. [27] reported that the *p*-aminohippurate transporter PAHT (synonym: hOAT1) [28], displayed an overshoot characterized by a time-dependent, saturable accumulation of substrate, followed by a gradual return to the baseline. In the current study, the uptake of *p*-[^{14}C]aminohippurate by HEK-hOAT1 also displayed this phenomenon (Fig. 1). OAT1 has been known as an organic anion/dicarboxylate exchanger [29], and it has been suggested that the overshoot is consistent with exchange-mediated secondary active transport in which an outwardly directed gradient for a cytosolic exchange partner (likely α-ketoglutarate) is depleted during the uptake experiment because of an abundance of the external exchange partner [27]. Recently, it was revealed that OAT3 is also an anion/dicarboxylate exchanger [30], and in the current study, the uptake of cefotiam by HEK-hOAT3 also displayed an overshoot. This is the first example of this phenomenon in hOAT3-mediated uptake after hOAT3 was recognized as an exchanger. In the uptake of cephaloridine by HEK-hOAT3, no overshoot was observed, although the uptake rate of cephaloridine was higher than that of cefotiam (2.08 μl/mg protein/15 min versus 0.72 μl/mg protein/15 min). Tune and Hsu [31] reported that cephaloridine reduces mitochondrial carnitine transport through competitive inhibition, and the zwitterionic region of this drug, like carnitine, is responsible for this ability. Given their study, it is suggested that cephaloridine was accumulated in mitochondria following its transport into the cytoplasm. Cytoplasmic concentration of cephaloridine may be low because intracellular cephaloridine was mainly in mitochondria. Therefore, the efflux of the antibiotic via hOAT3 was not occurred. We assume that this phenomenon also occurs in the proximal tubular cells, and participates in cephaloridine-induced renal failure.

We previously speculated that hOAT3 should play an important role in the secretion of cefazolin in patients with

renal diseases [14]. The current study demonstrated that other cephalosporin antibiotics are also secreted mainly via hOAT3. The uptake of cefoselis by HEK-hOAT3 was lower than the uptake of the other antibiotics, except for cefazolin, by HEK-hOAT3, and Sakamoto et al. [32] showed that cefoselis is mainly excreted by glomerular filtration. Accordingly, it should be that transport via hOAT3 is important for secretion in renal epithelial cells. It was reported that tubular secretion accounted for 50–80% of all the cefazolin excreted in patients with a glomerular filtration rate above 25 ml/min [33]. However, in the current study, the uptake of cefazolin by HEK-hOAT3 was lower than the uptake of the other antibiotics by HEK-hOAT3. The IC_{50} value of cefazolin for hOAT3 is remarkably lower than that of cefoselis for hOAT3 (116.6 μM versus 2925.1 μM). The protein-binding ratio of cefazolin (87%) is remarkably higher than that of cefoselis (8.8%) [32,33]. To elucidate the renal handling of drugs, it may be necessary to take such factors into consideration. We propose that information on transport via hOAT3 is, at least in part, useful for determining whether drugs can be secreted or not in renal epithelial cells.

In conclusion, hOAT3 plays a more important role than hOAT1 in the renal secretion of cephalosporin antibiotics. Furthermore, our findings provide useful information about the difference in substrate specificity between hOAT1 and hOAT3, and will contribute to further investigation of the renal handling of various drugs.

Acknowledgements

This work was supported in part by a grant-in-aid for Comprehensive Research on Aging and Health from the Ministry of Health, Labor and Welfare of Japan, by a grant-in-aid for Scientific Research from the Ministry of Education, Science, Culture and Sports of Japan, and by the 21st Century COE program "Knowledge Information Infrastructure for Genome Science."

References

[1] Burckhardt G, Wolff NA. Structure of renal organic anion and cation transporters. Am J Physiol Renal Physiol 2000;278:F853–66.
[2] Inui K, Masuda S, Saito H. Cellular and molecular aspects of drug transport in the kidney. Kidney Int 2000;58:944–58.
[3] Sekine T, Cha SH, Endou H. The multispecific organic anion transporter (OAT) family. Pflugers Arch 2000;440:337–50.
[4] Takeda M, Khamdang S, Narikawa S, Kimura H, Kobayashi Y, Yamamoto T, et al. Human organic anion transporters and human organic cation transporters mediate renal antiviral transport. J Pharmacol Exp Ther 2002;300:918–24.
[5] Khamdang S, Takeda M, Noshiro R, Narikawa S, Enomoto A, Anzai N, et al. Interactions of human organic anion transporters and human organic cation transporters with nonsteroidal anti-inflammatory drugs. J Pharmacol Exp Ther 2002;303:534–9.
[6] Hasannejad H, Takeda M, Taki K, Shin HJ, Babu E, Jutabha P, et al. Interactions of human organic anion transporters with diuretics. J Pharmacol Exp Ther 2004;308:1021–9.
[7] Motohashi H, Sakurai Y, Saito H, Masuda S, Urakami Y, Goto M, et al. Gene expression levels and immunolocalization of organic ion transporters in the human kidney. J Am Soc Nephrol 2002;13:866–74.
[8] Brown GR. Cephalosporin–probenecid drug interactions. Clin Pharmacokinet 1993;24:289–300.
[9] Yamazaki I, Shirakawa Y, Fugono T. Comparison of the renal excretory mechanisms of cefmenoxime and other cephalosporins: effect of *para*-aminohippurate on renal clearance and intrarenal distribution of cephalosporins in rabbits. J Antibiot 1981;34:1476–85.
[10] Takano M, Okano T, Inui K, Hori R. Transport of cephalosporin antibiotics in rat renal basolateral membranes. J Pharm Pharmacol 1989;41:795–6.
[11] Nagai J, Takano M, Hirozane K, Yasuhara M, Inui K. Specificity of *p*-aminohippurate transport system in the OK kidney epithelial cell line. J Pharmacol Exp Ther 1995;274:1161–6.
[12] Uwai Y, Saito H, Inui K. Rat renal organic anion transporter rOAT1 mediates transport of urinary-excreted cephalosporins, but not of biliary-excreted cefoperazone. Drug Metab Pharmacokinet 2002;17:125–9.
[13] Takeda M, Babu E, Narikawa S, Endou H. Interaction of human organic anion transporters with various cephalosporin antibiotics. Eur J Pharmacol 2002;438:137–42.
[14] Sakurai Y, Motohashi H, Ueo H, Masuda S, Saito H, Okuda M, et al. Expression levels of renal organic anion transporters (OATs) and their correlation with anionic drug excretion in patients with renal diseases. Pharm Res 2004;21:61–7.
[15] Urakami Y, Akazawa M, Saito H, Okuda M, Inui K. cDNA cloning, functional characterization, and tissue distribution of an alternatively spliced variant of organic cation transporter hOCT2 predominantly expressed in the human kidney. J Am Soc Nephrol 2002;13:1703–10.
[16] Bradford MM. A rapid and sensitive method for the quantitation of microgram quantities of protein utilizing the principle of protein–dye binding. Anal Biochem 1976;72:248–54.
[17] Hosoyamada M, Sekine T, Kanai Y, Endou H. Molecular cloning and functional expression of a multispecific organic anion transporter from human kidney. Am J Physiol 1999;276:F122–8.
[18] Cha SH, Sekine T, Fukushima J, Kanai Y, Kobayashi Y, Goya T, et al. Identification and characterization of human organic anion transporter 3 expressing predominantly in the kidney. Mol Pharmacol 2001;59:1277–86.
[19] Takeda M, Narikawa S, Hosoyamada M, Cha SH, Sekine T, Endou H. Characterization of organic anion transport inhibitors using cells stably expressing human organic anion transporters. Eur J Pharmacol 2001;419:113–20.
[20] Uwai Y, Okuda M, Takami K, Hashimoto Y, Inui K. Functional characterization of the rat multispecific organic anion transporter OAT1 mediating basolateral uptake of anionic drugs in the kidney. FEBS Lett 1998;438:321–4.
[21] Zhang L, Gorset W, Washington CB, Blaschke TF, Kroetz DL, Giacomini KM. Interactions of HIV protease inhibitors with a human organic cation transporter in a mammalian expression system. Drug Metab Dispos 2000;28:329–34.
[22] Atkinson RM, Currie JP, Davis B, Pratt DA, Sharpe HM, Tomich EG. Acute toxicity of cephaloridine, an antibiotic derived from cephalosporin C. Toxicol Appl Pharmacol 1966;8:398–406.
[23] Tune BM, Fernholt M, Schwartz A. Mechanism of cephaloridine transport in the kidney. J Pharmacol Exp Ther 1974;191:311–7.
[24] Tune BM. Nephrotoxicity of beta-lactam antibiotics: mechanisms and strategies for prevention. Pediatr Nephrol 1997;11:768–72.
[25] Takeda M, Tojo A, Sekine T, Hosoyamada M, Kanai Y, Endou H. Role of organic anion transporter 1 (OAT1) in cephaloridine (CER)-induced nephrotoxicity. Kidney Int 1999;56:2128–36.
[26] Jung KY, Takeda M, Shimoda M, Narikawa S, Tojo A, Kim DK, et al. Involvement of rat organic anion transporter 3 (rOAT3) in cephalor-

idine-induced nephrotoxicity: in comparison with rOAT1. Life Sci 2002;70:1861–74.
[27] Lu R, Chan BS, Schuster VL. Cloning of the human kidney PAH transporter: narrow substrate specificity and regulation by protein kinase C. Am J Physiol 1999;276:F295–303.
[28] Cihlar T, Lin DC, Pritchard JB, Fuller MD, Mendel DB, Sweet DH. The antiviral nucleotide analogs cidofovir and adefovir are novel substrates for human and rat renal organic anion transporter 1. Mol Pharmacol 1999;56:570–80.
[29] Sweet DH, Wolff NA, Pritchard JB. Expression cloning and characterization of ROAT1. The basolateral organic anion transporter in rat kidney. J Biol Chem 1997;272:30088–95.
[30] Sweet DH, Chan LM, Walden R, Yang X, Miller DS, Pritchard JB. Organic anion transporter 3 (Slc22a8) is a dicarboxylate exchanger indirectly coupled to the Na^+ gradient. Am J Physiol 2003;284:F763–9.
[31] Tune BM, Hsu C. Toxicity of cephaloridine to carnitine transport and fatty acid metabolism in rabbit renal cortical mitochondria: structure–activity relationships. J Pharmacol Exp Ther 1994;270:873–80.
[32] Sakamoto H, Hatano K, Higashi Y, Mine Y, Nakamoto S, Tawara S, et al. Animal pharmacokinetics of FK037, a novel parenteral broad-spectrum cephalosporin. J Antibiot 1993;46:120–30.
[33] Brodwall EK, Bergan T, Orjavik O. Kidney transport of cefazolin in normal and impaired renal function. J Antimicrob Chemother 1977;3:585–92.